Evidence for climate shifts in the ~2.0 Ga upper Makgabeng Formation erg, South Africa

Elizabeth A. Heness [1‡], Edward L. Simpson[1*], Adam J. Bumby[2], Patrick G., Eriksson[2], Kenneth A. Eriksson[3], Hannah L. Hilbert-Wolf[4], O. J. Okafor[2], Sarah Linnevelt[2], H. Fitzgerald Malenda[1], Tshepiso Modungwa[2]

[1]Department of Physical Science, Kutztown University, 425 Boehm, P.O. Box 730, Kutztown, PA 19530, ehene946@live.kutztown.edu,

[2]Department of Geology, University of Pretoria, Pretoria, 0002, South Africa,

[3]Department of Geosciences, Virginia Tech, 4044 Derring Hall, Blacksburg, VA 24061

[4]School of Earth and Environmental Sciences, James Cook University, Townsville, Qld 4811, Australia

*Corresponding author. Tel.: +1 610 683 4445; fax: +1 610 683 1352

‡Present Address: Department of Geological Sciences, University of Texas – El Paso, El Paso, TX 79968

email addresses: ehene946@live.kutztown.edu (E. Heness), simpson@kutztown.edu (E. Simpson), adam.bumby@up.ac.za (A. Bumby), Pat.Eriksson@up.ac.za (P. Eriksson), kaeson@vt.edu (K. Eriksson), Hilbert-Wolf (hannah.hilbertwolf@my.jcu.edu.au), Okafor (ojude12@yahoo.com), Sarah Linnevelt (sarah.linnevelt@favebook.com), H. Fitzgerald Malenda (hfm213@lehigh.edu), Tshepiso Modungwa (100000982997@facebook.com)

Highlights

- Syndepositional, normal faults created two sag ponds in the Wahweap Formation.
- Sag ponds record different histories of extension.
- Differences in sag pond fauna reflect different fill chronologies.
- Ancient sag pond deposits are useful for unraveling fault histories.

Graphical abstract

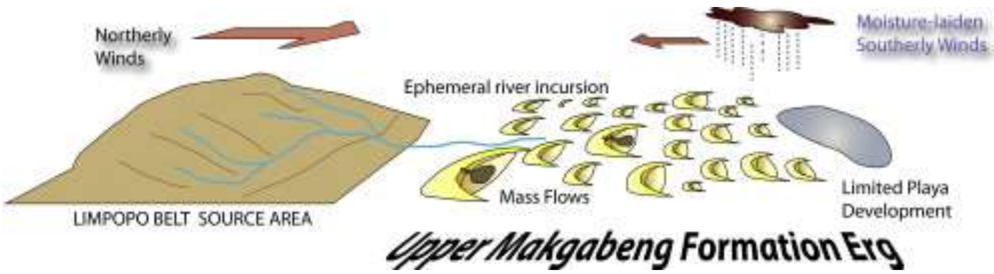

ABSTRACT

Eolian ergs, and associated environs are sensitive to short- and long-term climate changes. In one of the oldest, erg deposits, the ~2.0 Ga Makgabeng Formation, facies association changes reflect one of the earliest recordings of short-term climatic shifts in a continental setting.

The Makgabeng Formation is separated into lower and upper erg deposits by a playa or saline pan deposit. The lower erg deposit consists of dune sets with thin lenses of dry and deflationary interdunes that transitions vertically to thicker damp to wet interdunes. A laterally persistent playa deposit in the middle of the section consists of mudstone with deep and shallow penetrating mud cracks and subordinate siltstone and sandstone interbeds. Above this lower mudstone interval, the playa strata are sandy. Overlying the playa deposit, the upper erg deposit consists of thick eolian sets with thin lenses of dry interdune deposits. Grain size change near the top of the upper erg deposit corresponds to the appearance of fluvial, sheet flood, eolian cross-beds sculpted by mass flows, and thin playa deposits.

The vertical facies association demonstrates shifts in precipitation and fluctuating water tables. Fluvial and playa deposits record high water tables whereas low-water tables are reflected in the core erg. The transition from a lower to higher water table is recorded by wet interdune interspersed within the dune strata towards the top of this interval. Rapid climatic amelioration occurred near the termination of the Makgabeng erg resulting in impingement of ephemeral river systems, development of playas, and generation of massive sand flows. This 2.0 Ga erg demonstrates the impact of climate change on erg development, resulting from shifts in the monsoonal impingement through time.

KEY WORDS: Eolian, Paleoproterozoic, Playa, Ephemeral river, Makgabeng Formation

Introduction

Eolian dune fields, ergs, and associated environs are extremely sensitive to and impacted by short- and long-term climate changes commonly reflected in variations in precipitation (Parrish and Peterson, 1988; Peterson, 1988; Kocurek, 1991; Lancaster, 1997, Chan and Archer, 1999, 2000; Kocurek and Lancaster, 1999; Loope et al., 2001, 2004; Marín et al., 2005; Stone et al., 2010).

With the possible exception of inferred biocrust development, continental platforms probably were not characterized by the development of extensive terrestrial ecosystems during the Precambrian (Dott, 2003; Eriksson et al., 2013). Therefore, wind and water were more efficient in mobilizing sediment on the early continental Earth compared to modern continental settings. Supporting this assertion is the predominance in the Precambrian to Early Cambrian sedimentary record of braided-stream deposits. Because of the absence of significant root stabilization, sediment was easily eroded during precipitation events causing bedload transport to predominate (Cotter, 1978; Davies and Gibling, 2010a, 2010b; Long, 2011; Eriksson et al., 2013).

The oldest identified eolian dune field is reported from the 3.2 Ga Moodies Group of the Barberton Greenstone Belt, southeastern South Africa, a probable coastal-marine setting (Simpson et al., 2012). The Paleoproterozoic Makabeng Formation is considered to be one of the oldest substantial erg deposits (Eriksson and Cheney, 1992; Eriksson and Simpson, 1998; Simpson et al., 2004; Eriksson et al., 2013). Only broad descriptions exist concerning the Makabeng Formation erg (Callaghan et al., 1991; Eriksson and Cheney, 1992; Bumby 2000) and only specific facies associations have been described such as massive sand flows (Simpson et al., 2002), playa or saline pan deposits (Simpson et al., 2004), and continental microbial mats (Eriksson et al., 2000, 2007; Porada and Eriksson, 2009; Simpson et al., 2013).

This paper describes and interprets the various facies associations in the Paleoproterozoic Makgabeng Formation, reports on the vertical and horizontal distribution of facies associations, discusses the paleoclimatic implications of the vertical facies association stacking patterns, and documents one of the oldest examples in Earth's history of climatic change impact on erg evolution in a pre-Silurian dry land system.

1. Geological Setting

The Makabeng Formation is one of eleven formations comprising the Waterberg Group in the main Waterberg Basin and is preserved in a series of structural basins in South Africa (Figs. 1B and 2; SACS, 1980; Jansen, 1982; Walraven and Hattingh, 1993

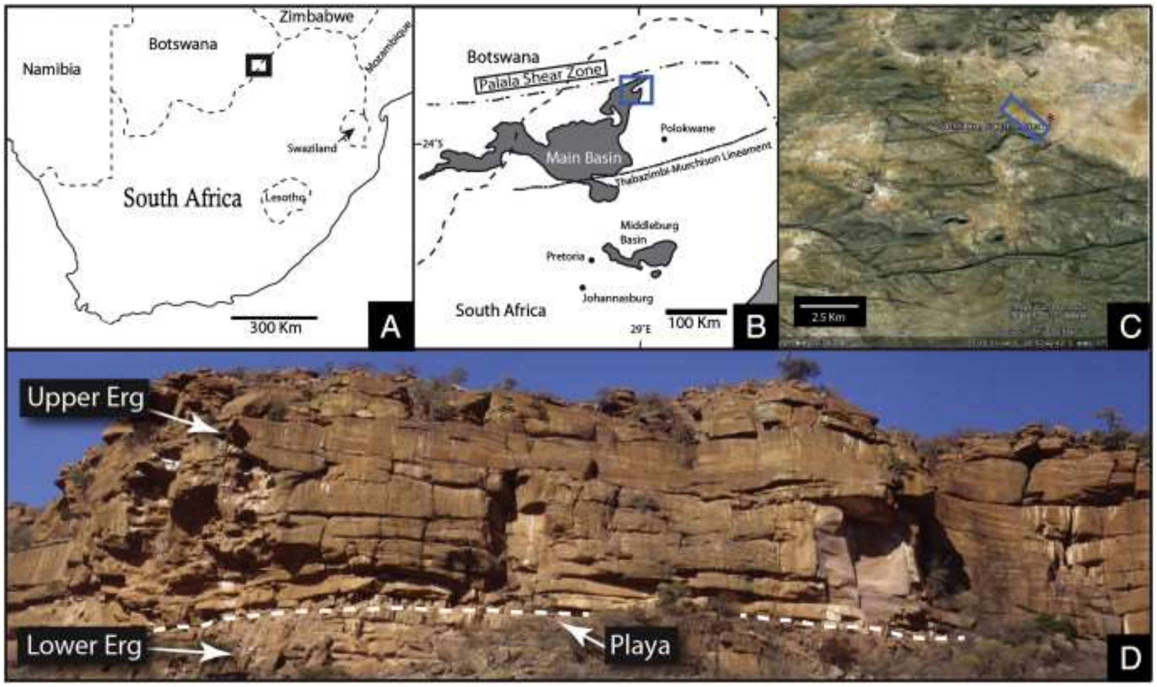

Fig. 1. A) Location of the study area in South Africa. Bold square highlights position of B. B) Location of Waterberg and Middelburg basins. Note the bounding structural features: Thabazimbi-Murchison Lineament and the Palala shear zone of the Limpopo Belt. C) Google Earth image of the Makgabeng Plateau and cliff face. Note the cross cutting lineations that represent dolerite dikes. Box marks the position of D. D) Photomosaic of the cliff face. Note the subdivision of the lower and upper dune field facies and the location of the playa facies. Height of the cliff face is approximately 35 m.

Bumby 2000; Bumby et al., 2001, 2004; Eglington and Armstrong, 2004; Hanson et al., 2004, Eriksson et al., 2006). The Main Waterberg Basin is bounded to the north by the Palala Shear Zone, which separates the Central Zone of the Limpopo Belt from the northern edge of the Kaapvaal Craton (Southern Marginal Zone of the Limpopo Belt) and to the south by the Thabazimbi-Murchison lineament (Fig. 1B; Light, 1982; Roering et al., 1992; Kröner et al., 1999). The Limpopo Belt had a protracted, complex tectonic history with numerous orogenic periods characterized by fault reactivation that acted as a northern source for sediment pulses entering and filling the Waterberg Basin (Fig. 1B;

Bumby, 2000; Bumby et al., 2001, 2004; Barton et al., 2006; Corcoran et al., 2013). Regional paleocurrent analysis supports a persistent source of detritus from the Limpopo Belt for the geological time span of the upper Waterberg Group fluvial systems (Callaghan et al., 1991; Bumby, 2000; Bumby et al., 2001, 2004; Eriksson et al., 2006, 2008). Recently, Corcoran et al. (2013) examined the petrology, major and trace element geochemistry, and U-Pb detrital zircon geochronology of the Waterberg Group and identified specifically the central Limpopo Belt as the source for the bulk of the sediment.

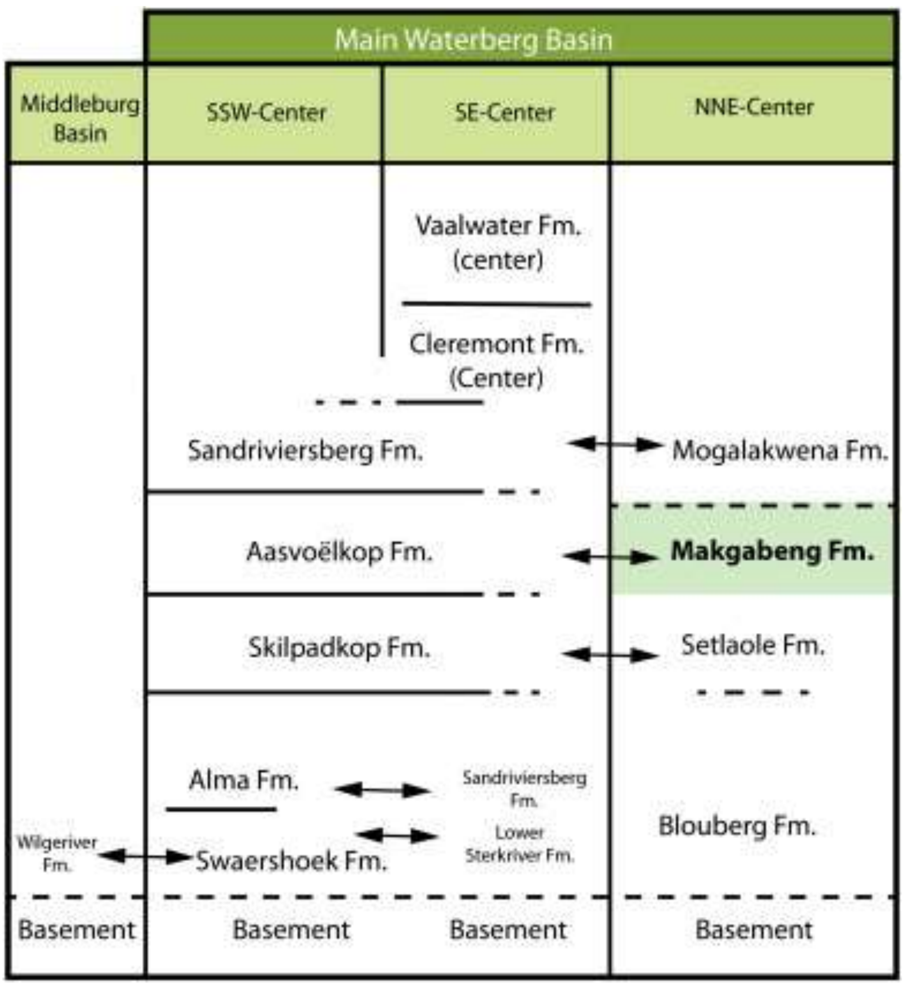

Fig. 2. Correlation chart of stratigraphic units of the Main Waterberg Basin and the Middelburg Basin. (Modified from Eriksson et al., 2008). Stratigraphy of the study are is in the NNE-Center column.

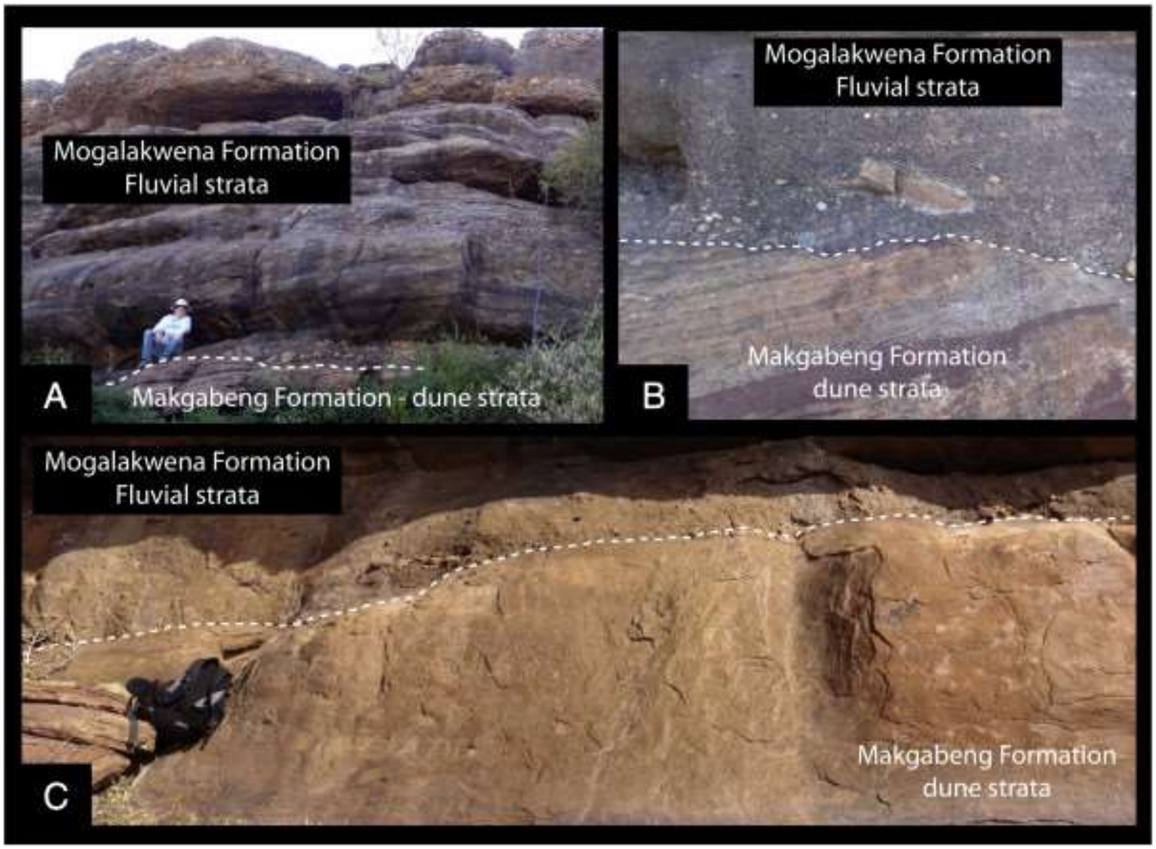

Fig. 3. Field photographs of the disconformable contact between the Makgabeng Formation and Mogalakwena Formation. A) Disconformable contact between eolian dune strata of the Makgabeng Formation and fluvial strata of the Mogalakwena Formation. Note the presence of thick conglomerates above the basal contact. B) Enlargement of the contact. Note the clast of Makgabeng Formation included in the Mogalakwena Formation. Coin is 20 mm in diameter. C) Erosive base of sandstone of the lowermost Mogalakwena Formation. Note backpack for scale.

In the northern part of the Main Waterberg Basin, sublithic sandstones of the Makgabeng Formation conformably overlie the Setlaole Formation and are, in turn, unconformably overlain by the Mogalakwena Formation (Figs. 2 and 3; SACS, 1980; Jansen, 1982; Bumby 2000; Corcoran et al., 2013). The Setlaole Formation consists of feldspathic sandstones and conglomerates that record southward-draining, braided-fluvial systems shed off the reactivated Limpopo Belt (Fig. 2; Callaghan et al., 1991; Bumby,

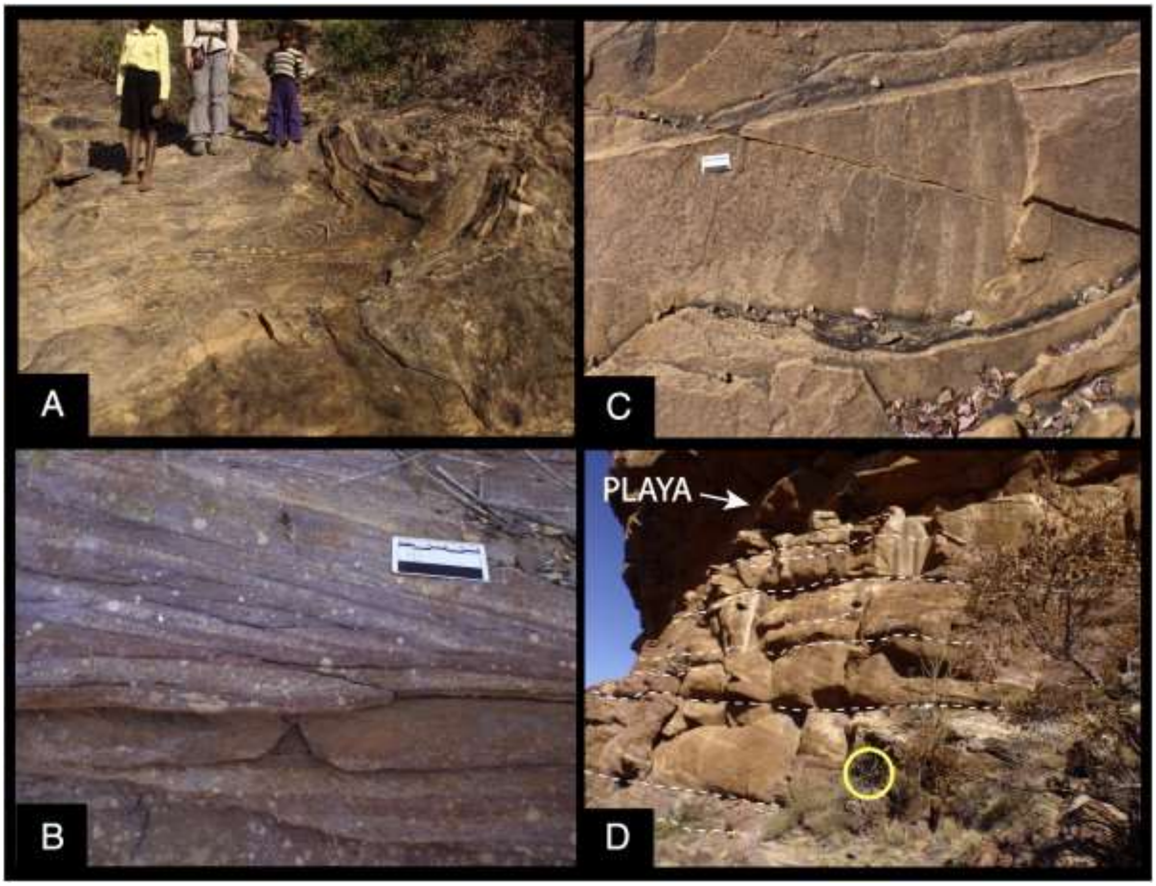

Fig. 4. Field photographs. A) Soft-sediment deformed Makgabeng Formation adjacent to a dolerite dike. Makgabeng Formation adjacent to the dike is more bleached of iron and heavily cemented with SiO_2. B) Sand or grain flows. Note that strata taper to the right. Grain flows are separated by grain fall stratification. C) Preserved wind-ripple bedforms on a cross bed foreset. Wind ripple bedform crests are orientated parallel to the dip direction of the foresets. Note the straight crest orientation and the even spacing of the wind ripples. Black bar on the photo scale is 5 cm. D) Field photograph of lower erg facies association. Cut is near parallel to the wind direction. Playa facies are located approximately at the overhang. Note backpack for scale, yellow circle.

2000; Bumby et al., 2001; Corcoran et al., 2013). The contact between the Setlaole and the Makgabeng Formation is not well exposed in the study area and possibly is gradational. Polymicitic conglomerates and subfeldspathic to sublithic sandstones characterize the younger Mogalakwena Formation and record the presence of significant braided stream systems with unusually high stream gradients and an absence of preserved overbank deposits (Eriksson et al., 2006; 2008). Again, the reactivated Limpopo Belt acted as a source (Eriksson et al., 2006, 2008; Corcoran et al., 2013).

The age of the Waterberg is constrained by U–Pb zircon ages of 2054±4 Ma and 2051±8 Ma from lavas in lower Swaershoek and Rust de Winter formations, located at the base of the Waterberg Group and potentially correlative with the Blouberg Formation (Fig. 2; Dorland et al., 2006), and U-Pb ages of ~1.92 - ~1.87 Ga from dolerite dikes that cross-cut the Mogalakwena Formation (Hanson et al., 2004) (Fig. 1C). The strata of the Makgabeng Formation adjacent to the dolerite dikes display soft-sediment folding and more significant diagenesis than the remainder of the Makgabeng Formation (Fig. 4A).

2. **Description of Facies Associations**

The Makgabeng Formation examined in this study is exposed along a cliff face, on the dip-slope plateau, and in additional erosional outliers (Figs. 1C and D). Multiple stratigraphic sections were measured and described along the Makgabeng cliff face (Fig. 1D). Grain size distribution, lithology, vertical and horizontal distribution of sedimentary structures and paleocurrent directions were recorded in the field for: 1) erg, 2) interdune, 3) playa, 4) ephemeral river and 5) mass flows (Figs. 5 and 6).

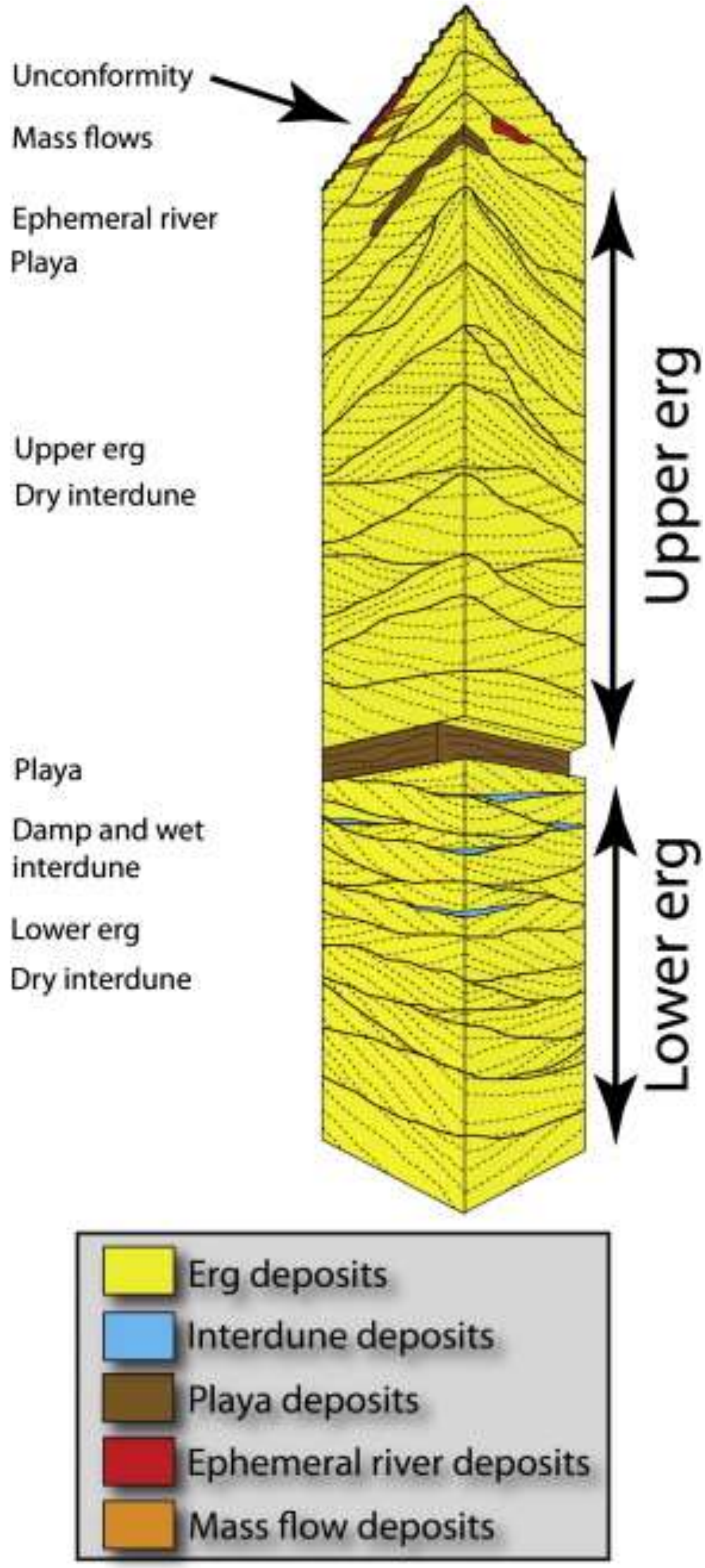

Fig. 5 – Generalized stratigraphic section showing the vertical distribution of facies associations.

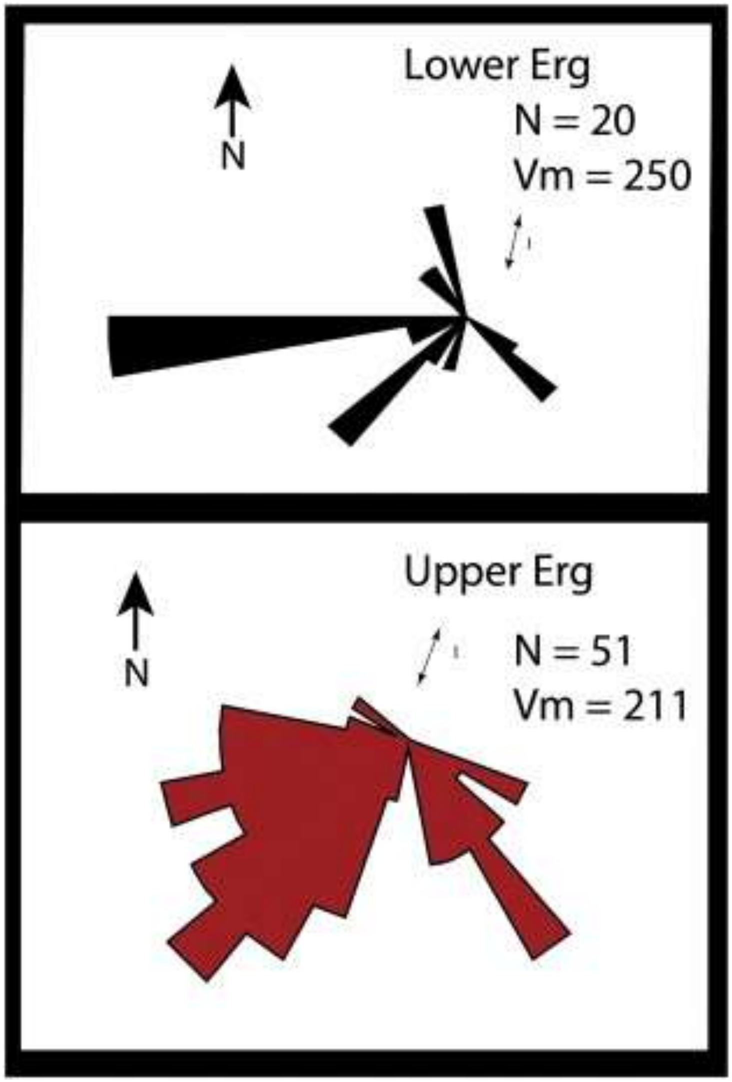

Fig. 6. Paleocurrent rose diagrams for the upper and lower erg. Note the overall trend is to the general southwest.

2.1 Erg Facies Association

2.1.1 Description

This facies association is best exposed on the cliff face and the plateau dip slope (Fig. 1). The erg facies association is developed in lower and upper units separated by the heterolithic playa facies association. The lower unit of erg facies association is approximately 40 meters thick; the lower contact is obscured in the study area. The upper unit of the erg facies association is approximately 80 m thick or more.

Strata in this facies association consist of hematite-stained, medium-grained sandstone containing inversely graded strata, grain flows, and grain falls (Figs. 4B and 4C), although recognition of grain fall strata is problematic. Cross beds are composed predominantly of wind-ripple strata with lesser proportions of grain flows (Fig. 4B). Grain flows pinch down the cross strata and are lens-shaped in bedding plane view (Fig 4B). Some inversely graded foresets possess low-relief asymmetrical bedforms with crest long axes oriented parallel to the maximum foreset dip (Fig. 4C).

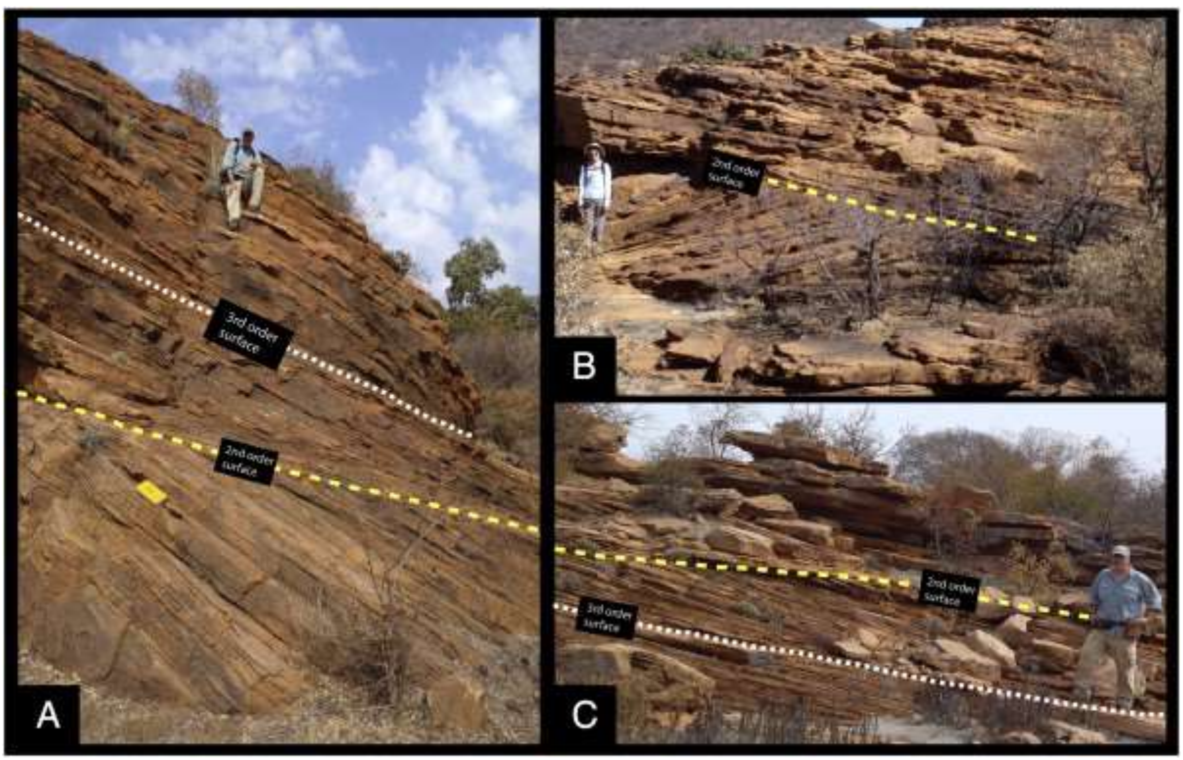

Fig. 7. Field photographs of the upper erg. A) Large foresets separated by a 2nd-order surface. Upper set has a 3rd-order surface overlain by downlapping foresets. Figure is 1.78 m tall. B) Apparent bidirectional foresets separated by a 2nd-order surface. Figure is 1.70 m tall. C) 2nd-order surface with a low angle 3rd-order surface. Figure is 1.78 m tall.

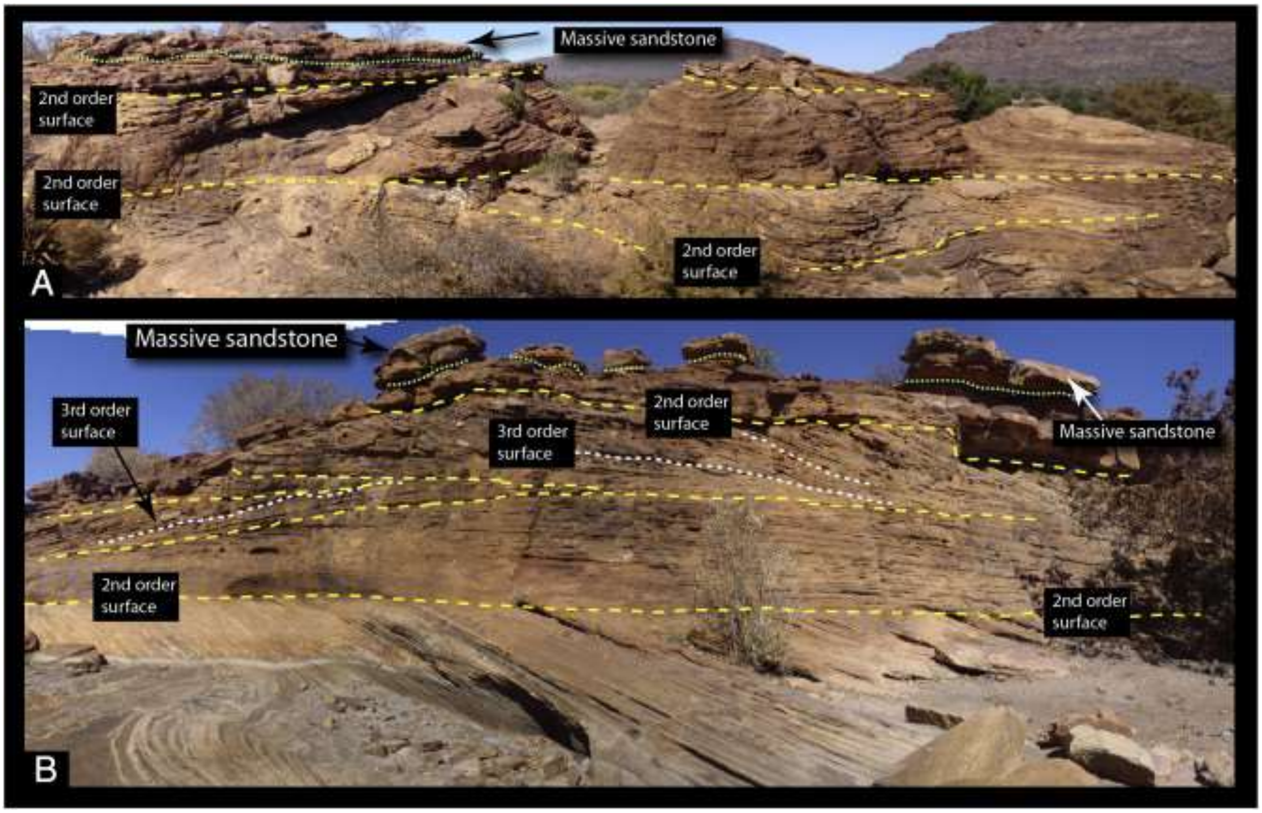

Fig. 8. Photomosaics of the upper erg on the Makgabeng Plateau. Both photos are near the contact with the Mogalakwena Formation. Massive sandstones are present within the top of A. White dashed lines are 3rd-order surfaces. Yellow dashed lines are 2nd-order surfaces.

Cross bed sets are up to 6 m in thickness (Fig. 7) and are tabular or lenticular to wedge-shaped in cross-section. Limited paleocurrent measurements of foresets along the cliff face in the lower erg are directed towards the south-southwest (Fig 6A). Paleocurrent vector measurements on the plateau from the upper erg indicate a mainly south-southwest direction (Fig. 6B). Within the cross beds, a hierarchy of bounding surfaces is developed. Rare 3rd-order surfaces truncate and are downlapped by the various stratification types. Second-order surfaces truncate 3rd-order surfaces. Third-order surfaces are present and better developed in the upper than the lower erg facies association (Figs. 7, and 8). Near the contact with the Mogalakwena Formation, wedge-shaped massive sandstones are developed at the bases of cross bed sets and onlap some 3rd-order surfaces. Second-order surfaces lower in the section are planar and continuous whereas near the top of the section trough- and wedge-shaped surfaces predominate.

2.1.2 Interpretation

The predominance of wind-ripple strata characterized by inverse grading, coupled with the presence of grain flows and grain fall in the erg facies association are consistent with stratification types and processes described from modern eolian dunes in the seminal work of Hunter (1977, 1981) and Kocurek and Dott (1981). Third-order surfaces develop from fluctuating wind directions and velocities that rework the dune lee face (Brookfield, 1977; Kocurek, 1981, 1991). The paucity of 3rd-order surfaces in the lower erg facies association implies a consistent wind direction (Kocurek, 1981). Erosion generated from flow reattachment on the stoss side of the preceding climbing dunes generated the 2nd-order bounding surfaces. The bounding surface geometry was controlled by the original dune morphology and potentially by a variety of other factors such as sediment supply, climate, water table position, and basin subsidence (Wilson, 1972; Brookfield, 1977; Kocurek, 1981, 1991; Rubin and Hunter, 1982; Clemmensen and Blakely, 1989; Mountney et al., 1999; Rubin and Carter, 2006). Geometry of the foresets and bounding surfaces within the Makgabeng Formation is consistent with barchan and barchanoid to transverse dune types (Meinster and Tickell, 1975; Callaghan et al., 1991; Bumby, 2000; Eriksson et al., 2000)

Measured paleocurrent data (Fig. 6) are consistent with previous reports of strong, southerly directed paleowinds for the Makgabeng Formation (Callaghan et al., 1991; Bumby, 2000).

2.2 Interdune Facies Association

2.2.1 Description

The interdune facies association is best developed in the upper 25 meters of the lower erg and near the top of the upper erg. Interdune strata are lenticular in shape and

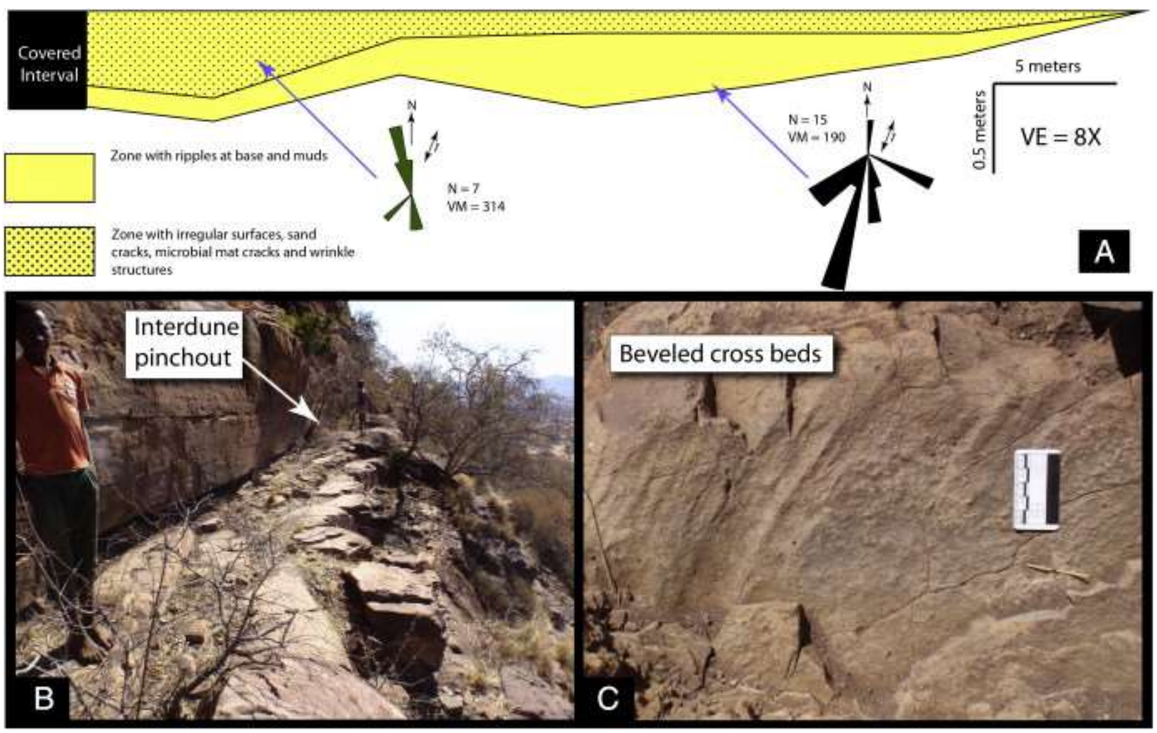

Fig. 9. Interdune facies. A) Geometry and internal stratigraphy of interdune deposit. Paleocurrent rose diagrams demonstrate variability in the orientation of the paleocurrents in the interdune area. B) Outcrop of interdune deposit through the vertical extent of the outcrop face. Lateral extent of the interdune deposit in the photograph is approximately 30 m. C) Bedding plane view of interdune edge showing beveled cross beds overlain by interdune deposit. Black bar on scale is 5 cm.

are traceable laterally for up to 75 m (Fig. 9). Maximum measured thicknesses are ~85 cm. The contact with underlying dune strata along the edge of the lens is sharp and beveled (Fig. 9C) whereas the overlying low-angle dune strata are in sharp to slightly undulatory contact with the interdune strata (Fig. 9A).

Sedimentary structures developed within the interdune facies association are ripple bedforms including symmetrical and slightly asymmetrical to asymmetrical forms with vertically accreting symmetrical ripples and form-concordant drapes in cross section (Fig. 10). Asymmetrical ripple bedforms are lunate to cuspate in plan view. On bedding plane exposures, bedforms vary laterally from slightly to strongly asymmetrical (Figs. 10A and 10C). Symmetrical ripple stratification styles dominate the upper portions of the interdune deposit (Fig. 10B). Numerous beds that are capped by ripple bedforms display complex desiccation patterns and isolated spindle-crack features (Fig. 10F; Eriksson et al., 2000, 2007; Porada and Eriksson, 2009; Simpson et al., 2013). Additional features present within the interdune facies association include muddy roll-up structures, gas-escape structures, graded beds, tufted mats, adhesion warts, raindrop impressions, desiccated mudstones, mud chips, and various morphologies of sand cracks (Fig. 10E; Simpson et al., 2013).

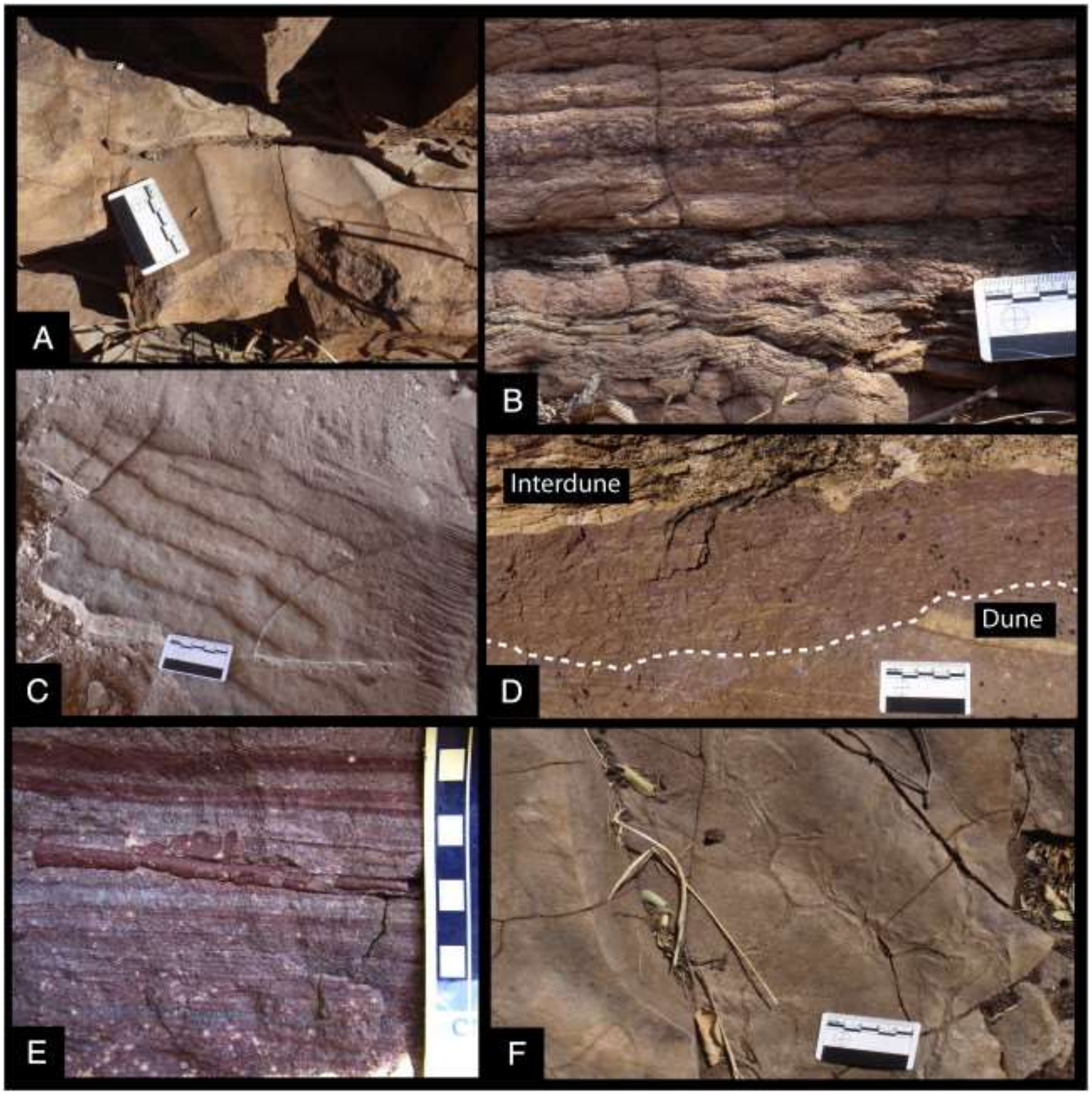

Fig. 10. Field photographs of ripple stratification in the interdune facies association. A) Symmetrical ripples. B) Cross section view of vertically accreting symmetrical ripples and form-concordant drapes. C) Slightly asymmetrical ripples. D) Cross section of erosively based, small-scale trough laminations overlying dune stratification. E) Longitudinal profile of muddy roll-up feature. Scale is in cm, F) Bedding plane view of desiccated sandstone. Black scale bar is 5 cm.

2.2.2 Interpretation

All reported features and bed geometries developed in this facies association have been reported previously from interdune deposits (e.g. Kocurek, 1981; Fryberger et al., 1983). Two end member conditions are interpreted to be represented by the Makgabeng Formation interdune deposits, dry or deflationary and damp/wet (Kocurek, 1981; Fryberger et al., 1983). Deflationary processes in interdune areas generate erosive 2nd-order surfaces as a result of sand transport across the interdune area (Brookfield, 1977; Kocurek, 1981, 1991). Low-angle to horizontal wind-ripple deposits resting on 2nd-order surfaces reflect dry interdune conditions characterized by wind-induced sediment transport and net sand aggradation within the interdune area (Kocurek, 1981; Fryberger et al., 1983). Deflationary and aggradational conditions, wind-ripple deposits, vary spatially across a single interdune area (Kocurek, 1981; Fryberger et al., 1983).

Water significantly impacts the generation of sedimentary structures characterizing wet interdune deposits (Gradziński et al., 1979; Kocurek, 1981; Fryberger et al., 1983; Pulvertaft, 1985; Lancaster and Teller, 1988; Gradziński and Uchman, 1994; Mountney and Jagger, 2004). Water movement in the Makgabeng interdune areas generated wave-, combined flow- and current-ripples recorded in symmetrical to strongly asymmetrical ripple bedforms and linked cross-sectional sedimentary structures such as vertically accreting symmetrical ripples and form-concordant drapes (*cf.* Harms el al., 1982; Allen, 1984). Muddy roll-up structures, gas-escape features, tufted mats, desiccated mudstones, mud chips, and various morphologies of sand cracks record thriving microbial mat communities that inhabited the damp and wet interdune areas (Eriksson et al., 2000, 2007; Porada ad Eriksson, 2009; Simpson et al., 2013). Additional sedimentary structures indicative of damp to wet conditions include graded beds, adhesion warts, raindrop impressions.

Wet interdune deposits are linked to the presence of a high water table and interdune ponds are sustained by consistently high water tables (Lancaster, 1997; Mountney and Jagger, 2004). The transition from a low to a higher water table in the Makgabeng Formation is recorded in the transition from thinner dry and deflationary to thicker damp and wet interdune deposits. In the Permian Cedar Mesa Formation damp and wet interdune deposits occur at the erg margin with dry and deflationary interdunes in the main dune core (Mountney and Jagger, 2004). In addition, within a single interdune deposit, Mountney and Jagger (2004) recognized that damp interdune deposits pinch out both parallel and perpendicular to the sand transport direction while wet interdune deposits were confined to trough bases and had limited lateral and vertical extent. In the Makgabeng setting, we infer that wet interdune deposits were generated by flooding of the interdune areas producing interdune ponds.

2.3 Playa/Saline Pan Facies Association

2.3.1 Description

Since the original interpretation in Bumby (2000) and Simpson et al. (2004), a collapse of the Makgabeng cliff outcrop has freshly exposed the playa facies association. The clean vertical face allows direct field observation enabling a more detailed interpretation of macroscopic structures as relied on by Simpson et al. (2004). The playa facies association is found in two different stratigraphic locations. The lower example of the playa facies association separates the upper and lower erg deposits and the upper example occurs below the contact with the overlying Mogalakwena Formation.

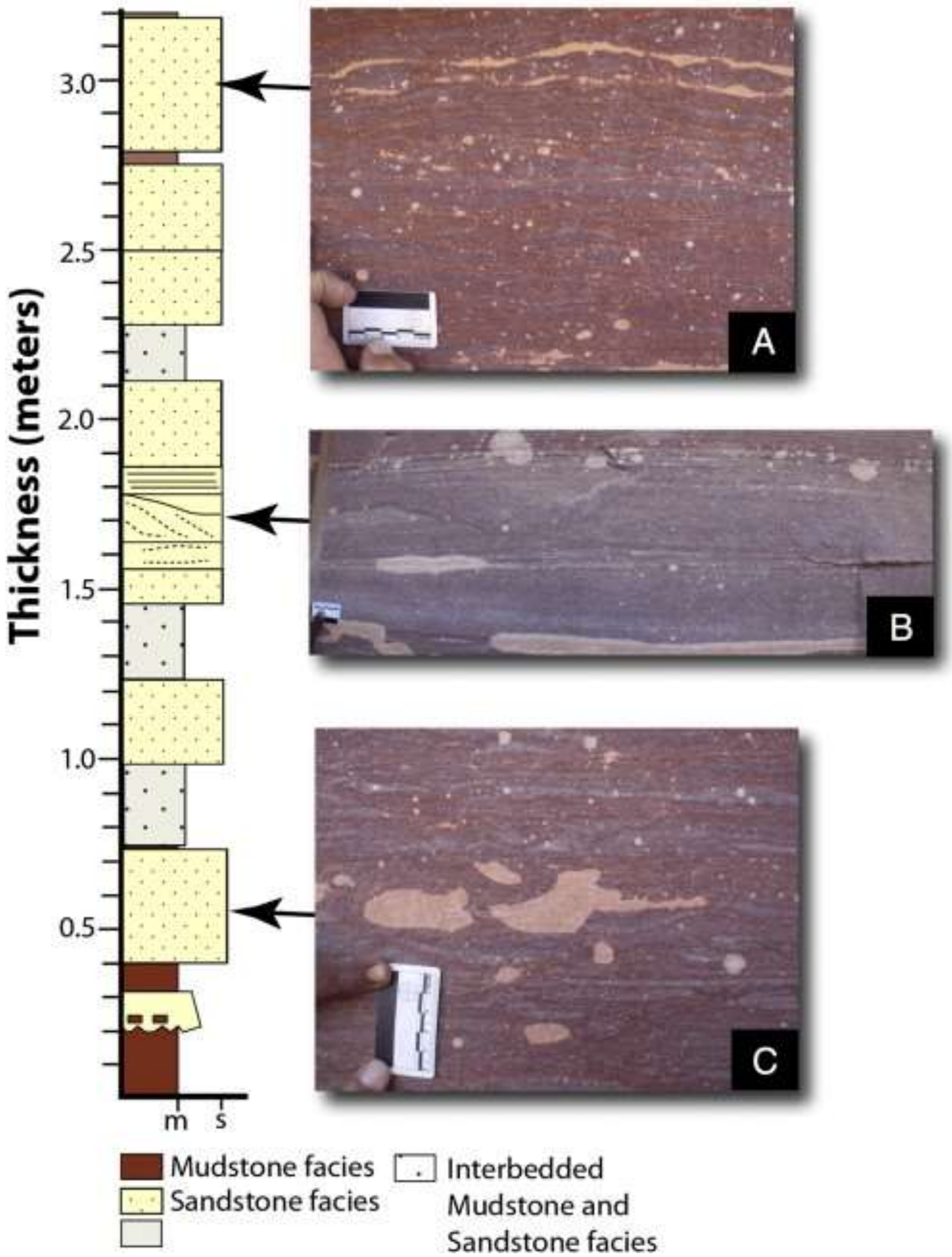

Fig. 11. Stratigraphic column of the lower playa deposit that separates the lower and upper erg deposits. Field photographs A-C. A) Interbedded sandstone and mudstone facies. B) Low–angle eolian stratification channelized and filled with massive sandstone. C) Sandstone dominated facies with reduction zones.

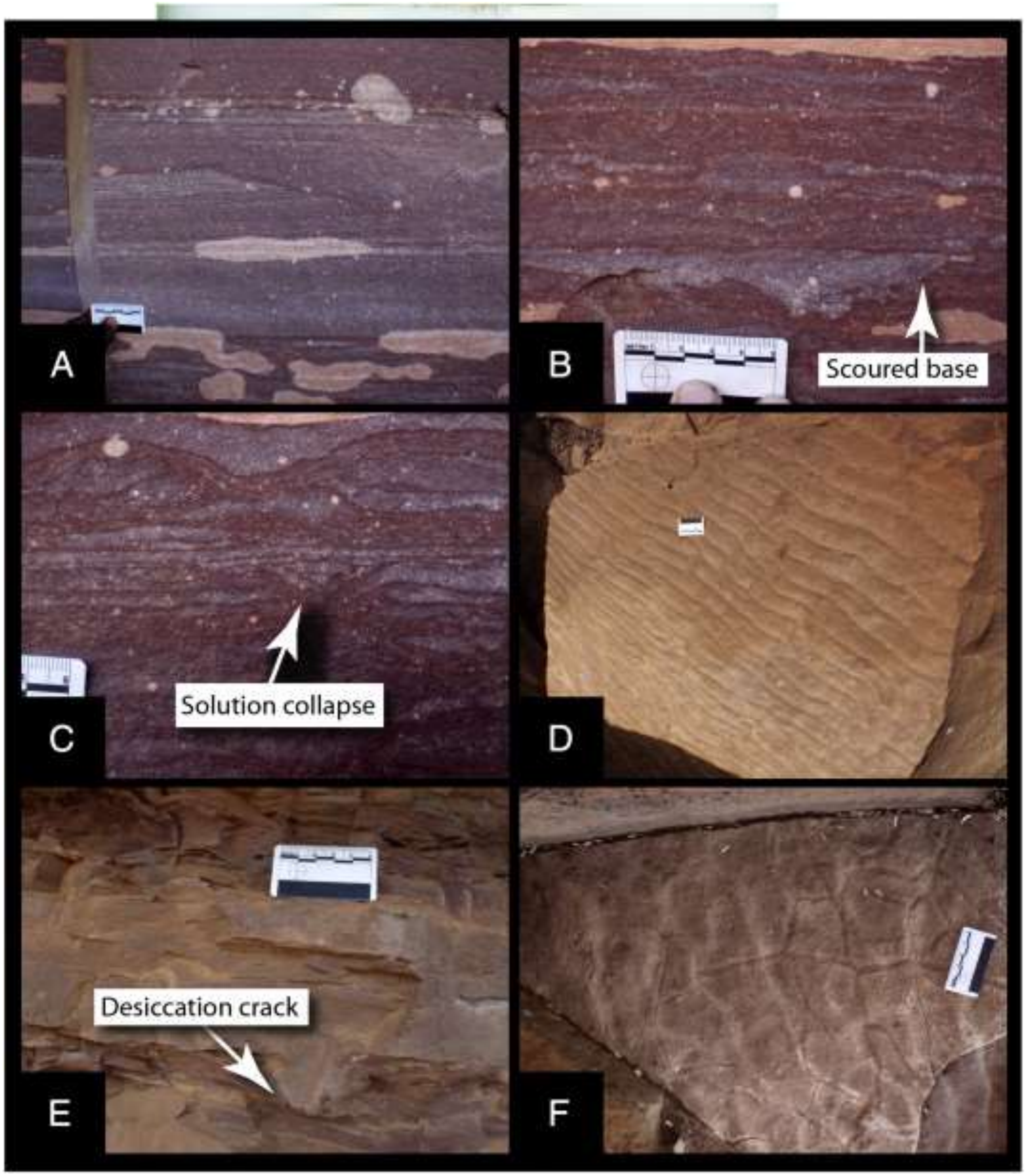

Fig. 12. Field photographs of the playa facies. A) Low-angle wind-ripple foresets. B) Scoured base overlain by a graded bed with intraclasts (See arrow). Note preserved ripple morphologies near the top of the photograph. C) Solution collapse feature at center and draped mounds near the top of the photograph. D) Preserved wave-ripple bedforms. Note the presence of small secondary wave ripples in the troughs. E) Large sand-filled desiccation cracks at the base of the playa (See arrow). F) Preserved current-ripple bedforms with superimposed sand cracks reflecting the former presence of microbial mats.

The lower playa deposit has a maximum thickness of 3.2 m (Fig. 11), whereas the upper playa deposit is 2.0 m. The lower playa deposit is traceable for over 1 km (Bumby, 2000). Within the playa facies association, three facies are recognized: mudstone, sandstone and an interbedded mudstone-sandstone facies (Fig. 11). The lower playa deposit contains all facies whereas the upper playa deposit is dominated by the sandstone facies (Figs. 11 and 12). Two thin mudstone layers delineate the boundary between the lower playa deposit and the upper erg deposit each less that 2 mm thick (Fig. 11).

At the transition from the lower erg to the lower playa deposit, patches of biological soil crust features are preserved (see Simpson et al., 2013). Mudstone facies that overlies the biological soil crust contains two to three 15-20 cm thick well-cemented sandstone interbeds alternating with graded siltstone and mudstone. In the eastern part of the playa exposure, the mudstones are crosscut by large desiccation cracks filled with sand from the overlying layer (Fig. 12E). Faint cross laminations are present at the base of the graded siltstone to mudstone facies. The well-cemented sandstones display desiccation cracks on their upper surfaces.

Above this lower mudstone facies, the playa deposit transitions abruptly into a more sand-dominated interval. Sandstone-dominated facies are distinguished from mudstone-sandstone facies based on the presence of thicker mudstone laminations (Fig. 12). Both facies have various proportions of wave-, combined flow, and current-ripples, horizontal to low-angle eolian wind-ripple stratification, scours at the base of the beds, graded beds, horizontally laminated beds and massive beds. In bedding plane view, double-crested wave-ripples, with lesser amplitude crests in the troughs (Fig. 12D), wave ripples, combined flow (Fig. 12D), and current ripples (Fig 12F) are identifiable.

Wind-ripple cross bed sets are present at 1.6 m from the base of the lower playa deposit (Fig. 11). This interval is recognizable throughout the extent of the playa along the cliff face. An erosively based, graded sandstone bed truncates the wind ripple cross strata (Figs. 11 and 12A). Foreset dip increases up the wind ripple set (Figs. 11D and 12A).

In addition to the above sedimentary structures, evaporitic crust features and evaporite dissolution structures are abundant. Collapse grabens were documented in Simpson et al. (2004). In fresh exposure, collapse features disturb strata up to 50 cm in thickness on a larger scale than previously recognized (Fig. 12B and 12C). At a smaller-scale, bump-like features are present in which fine-grained red mud layers create wavy structures in the heavily hematite-stained sandstone (Figs. 12B and 12C).

The upper playa is encased within the upper erg approximately 8 m below the contact with the Mogalakwena Formation. Within this sandstone facies, current to wave ripple bedforms are observed along with modified bump-like features capped by red mud layers (Fig. 13). In addition, low angle erosion surfaces are present with massive sandstone fills (Fig 13A).

Fig. 13. Field photomosaics of the upper playa. A) Sandstone facies in upper playa. Note the low-angle scours. B) Sandstone facies in the upper playa. Note the presence of climbing asymmetrical ripple bedforms in the upper-right quadrant. Black bar on scale is 5 cm.

2.3.2 Interpretation

The suite of sedimentary structures developed in this facies association is comparable to previously described playa or saline pan facies (Smoot and Castens-Seidell, 1994; Gierlowski-Kordesch and Rust, 1994; Turner and Smith, 1997; Benison and Goldstein, 2000; Bumby, 2000; Reinhardt and Ricken, 2000; Simpson et al., 2004). Biological soil crusts and microbial mat features in the lower playa deposit were recently described and interpreted in Simpson et al. (2013).

The mudstone facies represents the deepest-water phase and potentially the greatest lateral extent of the playa. The deepest part of the playa was impacted by sediment pulses recorded in the graded siltstone beds.

The various sedimentary structures in the sandstone and mudstone-sandstone facies are interpreted to have formed by evaporation, desiccation, flooding and wind action on surrounding playa flats (see Benison and Goldstein, 2000). Distinctive sedimentary structures in the Makgabeng playa deposit that mark the former presence of efflorescent salt crusts include surface deformation features, such as deformed ripples and solution collapse structures represented by solution loading and growth faulting (cf. Smoot and Castens-Seidell, 1994). Langston and McKenna Neuman (2005) demonstrated that evaporitic crusts weaken when subjected to mass transport events and eventually fail during transport. Evaporitic crusts along with biological soil crusts in the Makgabeng Formation are considered to have aided in the stabilization of the playa surface.

Smoot and Castens-Seidell (1994) observed that wind-blown dust hydroscopically adheres to the efflorescent crusts. Thinner crusts are found near the margins of the playas or saline pans and develop where the phreatic brine is deeper below the surface (Smoot and Castens-Seidell, 1994). Thin crusts are subject to rapid dissolution when flooded because they are in disequilibrium with both subsurface brines and rainwater (Smoot and Castens-Seidell, 1994). The amount of mud adhering to the crusts varies depending upon rainfall (Smoot and Castens-Seidell, 1994). Crusts that have experienced recent precipitation in areas subject to frequent flooding, and crusts that are buried rapidly have less mud trapped (Smoot and Castens-Seidell, 1994). This phenomenon is recorded in the Makgabeng playa deposit as variations in the thickness of mudstone draping bedforms.

Vertical stacking of the various playa facies reflects fluctuations in precipitation. Over longer time frames, flooding followed by desiccation is recorded in the lower playa mudstone (cf. Lowenstein and Hardie, 1985; Last, 1989). In contrast, efflorescent crust features are consistent with shorter period (months or years) flooding, followed by desiccation cycles (cf. Last, 2002; Simpson et al., 2004), and may reflect variations in seasonal precipitation as noted elsewhere by Turner and Smith (1997). Mudstone-rich accumulations on playa stratification may develop through the moisture trapping and aggradation of eolian dust (Holliday et al., 2008). Playa sediments can be reworked around the playa margins into barchans dunes (Handford, 1982). Sedimentary structures in the upper playa are consistent with a playa sand-flat setting (Handford, 1982) and may record a shorter interval of higher water table levels than in the lower playa deposit.

The laterally continuous layer with dune stratification in the middle of the lower playa represents either the development of an arid interval, or the initial encroachment of the younger erg. In the former case, this laterally extensive eolian interval would represent the development and limited preservation of small dunes before the encroachment of core erg (cf. Loope and Simpson, 1992).

2.4 Ephemeral River Facies Association

2.4.1 Description

Coarse-grained to pebbly sandstone occurs near the upper contact of the Makgabeng Formation with the overlying Mogolakwena Formation (Fig. 14). According to Bumby (2000), this facies association is up to 30 m thick. Modern-day erosional topography on the plateau limits observations of this facies association and thus the understanding of its lateral extent within the upper deposit. Vertical successions include horizontal stratification with parting lineation overlain by large- or medium-scale trough cross beds, followed by medium-scale trough cross beds (Fig. 14). Within the upper erg facies association, intervals of horizontal stratification overlain by medium-scale trough cross bedded sandstones are up to 3 m thick and are in erosional contact with underlying dune cross-strata (Fig. 19C). Clasts are 2 to 7 cm in diameter and consist of quartz and quartzite (Bumby, 2000). Channel forms range from 5 to 11 m wide and are scoured to depths of 0.5 to 0.7 m (Bumby, 2000). Paleocurrents measurements trend southward (Bumby, 2000).

Fig. 14. Field photographs of ephemeral river facies association. A) Parting lineation in horizontal stratification. Coin is 1.5 cm in diameter. B) Bedding plane view of large-scale cross-bedded pebbly sandstone facies. C) Vertical succession of horizontal stratification overlain by trough cross bedding overlain by horizontal stratification. Figure is 1.7 m tall.

2.4.2 Interpretation

The vertical succession of sedimentary structures in this facies association is consistent with deposition in bedload-dominated ephemeral braided stream systems (cf. Williams, 1971; Frostick and Reid, 1977; Allen, 1983; Bhattacharyya and Morad, 1993; Tooth, 2000; Bridge, 2003; Billi, 2007). These ephemeral systems drained from the

Limpopo Belt to the north and clast types, notably quartzite, can be related to lithologies in the Limpopo Belt (Bumby, 2000).

Ephemeral fluvial systems commonly introduce extrabasinal clasts into the erg (Svendsen et al., 2003) and fluvial incursion into eolian dunes fields has been documented by various workers (e.g. Langford, 1989; Langford and Chan, 1989; Terwin, 1993; Loope et al., 1995; Svendsen et al., 2003). The role of dune damming to induce local dune flooding and formation of lakes has been recognized (Loope et al., 1995; Svendsen et al., 2003). Water-saturated sands released from dam breaching are subject to bulking of normal type flow by eroding sand from the surrounding dunes thus modifying the hydrodynamics to those more akin to hyperconcentrated flows (Svendsen et al., 2003 and Simpson et al., 2002).

2.5 Mass Flow Facies Association

2.5.1 Description

Massive sandstones are restricted to the top of the upper erg deposit (Fig. 15; Simpson et al., 2002). Bases of massive sandstone bodies are channelized to planar with very low-angle to near vertical channel margins (Figs 15 B and 15C). Planar-based massive bodies are present above horizontal to low-angle dune toesets whereas channelized bodies are erosional into tops of cross bed sets (Fig. 8; Simpson et al., 2002). Massive sandstone bodies range in shape from tabular to lobate. Lobate bodies are to 6 m thick and from 3 m to possibly over 50 m in lateral extent (Simpson et al., 2002). Some massive sandstone bodies onlap 3rd-order surfaces within dune deposits and up to four have been recognized in succession within a single cross bed set. Other sedimentary

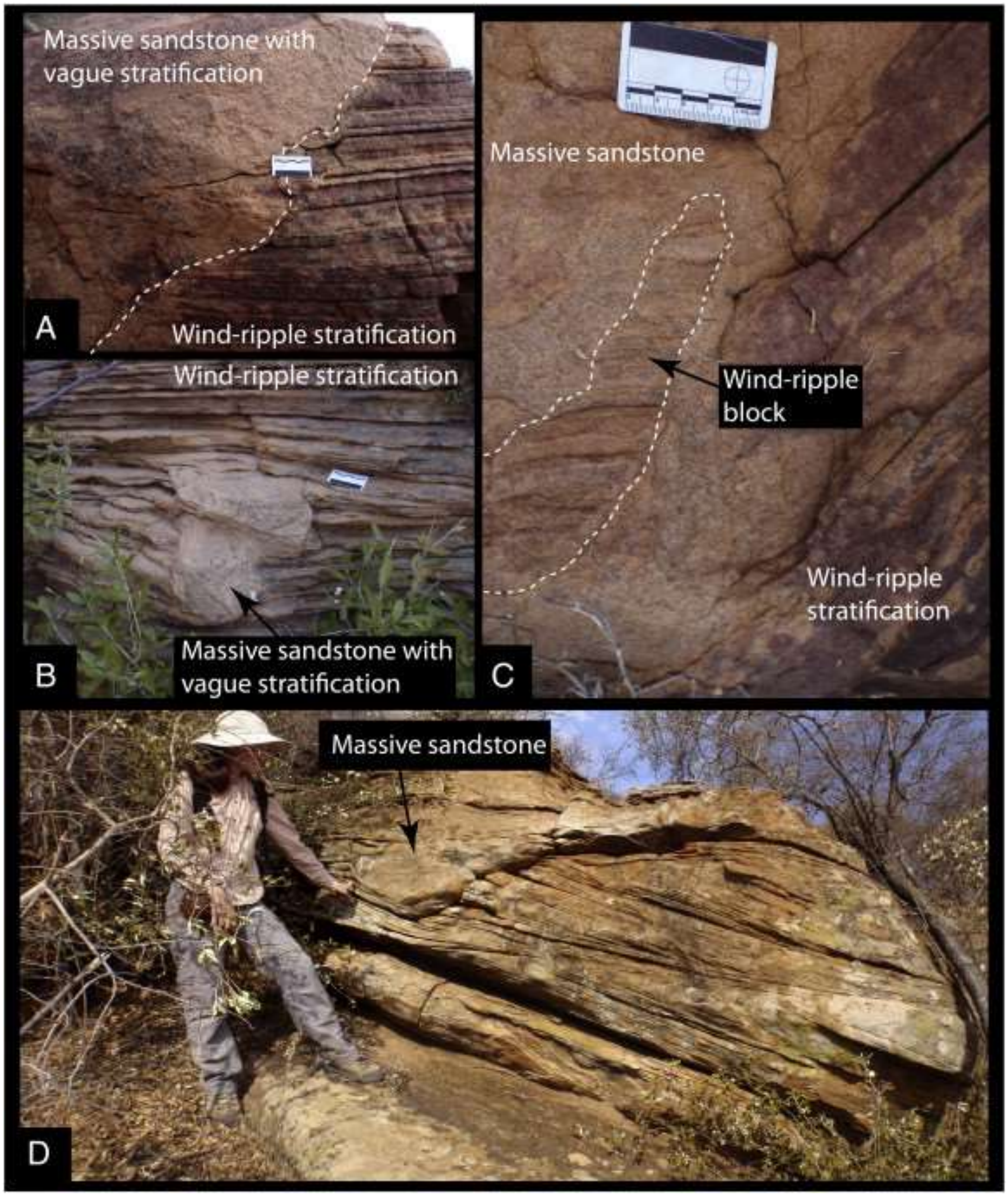

Fig. 15. Field photographs of the massive sandstone facies association. A) Erosively based massive sandstone facies with vague near horizontal stratification. Card is 5 cm. B) Near vertical-walled massive sandstone channel deposit capped by inclined stratification. Card is 5 cm. C) Vertical-walled massive sandstone channel deposit with included block of wind ripple stratification. Card is 5 cm. D) Channelized massive sandstone cut into underlying dune stratification. Dune stratification caps the massive sandstone. Figure 1.70 m in height.

structures associated with the massive sandstones are horizontal stratification, ripped-up fragments of wind-ripple strata (Fig. 15), rare dewatering features, parting lineations and capping adhesion warts (Simpson et al., 2002).

2.5.2 Interpretation

Massive sandstone in dune strata are triggered by intense precipitation events and are deposited from bulking by sediment sediment erosion. The resulting hyperconcentrated flows move down the dune lee face, sculpting the dune as a turbulent flow (Wizevich, 1997; Loope et al., 1998, 1999; Sweeny and Loope, 2001; Simpson et al., 2002). As the bulked hyperconcentrated flows migrate onto the dune plinth, rapid deposition produces lobate-shaped, massive sandstone deposits comparable to those described above, with some flows maintaining turbulence onto the dune plinth to produce the planar-based bodies in the Makgabeng Formation. Massive sandstone bodies draping 3^{rd}-order reactivation surfaces are interpreted as the result of partial lee-face collapse (Bumby, 2000; Simpson et al., 2002). The lateral repetition of the mass flow sandstone bodies along sets may reflect modification and recovery of the dune lee face from successive precipitation events (cf. Hunter and Richmond, 1988; Chan and Archer, 1999, 2000; Loope et al., 2001, 2004; Scherer and Goldberg, 2010).

3. Vertical Stacking of Facies Associations

The upper Makgabeng Formation is composed mainly of eolian stratification. Laterally extensive playa deposits separate the eolian strata of the lower and upper erg (Fig. 16). Subdivision of the Makgabeng Formation erg can be compared with the scheme of Porter (1986, 1987) who introduced the terms fore-erg, central-erg, and back-erg. Initial eolian sedimentation in the Makgabeng Formation is interpreted to record the fore-erg field characterized by zibars, small dune complexes, and sand-sheets. Wet interdune deposits are associated with the leading edge of the erg. Thick, large-scale eolian sets in the middle of the lower erg deposit represent the central-erg. Back-erg deposits are typically thin to absent in modern ergs depending on the conditions that led to termination of erg sedimentation. The transition from dry/deflationary interdune deposits to damp and wet interdune deposits at the top of the lower erg reflects a transition from the central-erg to the back-erg. The lower erg deposits are separated from the overlying playa deposits by an irregular erosional surface capped and stabilized by biological soil crusts. This surface represents a super-bounding surface and reflects interruption in dune sedimentation; dune deposits are preserved only on paleotopographic highs. Playa facies capping this surface record the maximum expanse and depth of the playa. The transition from the playa to the upper erg, the fore-erg is not preserved and may be recorded in the upper part of the playa facies association by the presence of the extensive eolian interval. The base of the upper erg overlies the lower playa deposit and signifies the recurrence of the central-erg. Near the top of the upper erg, the presence of smaller sand-dominated playa deposits, massive sandstones sculpting dune stratification, and ephemeral river deposits records the back-erg setting.

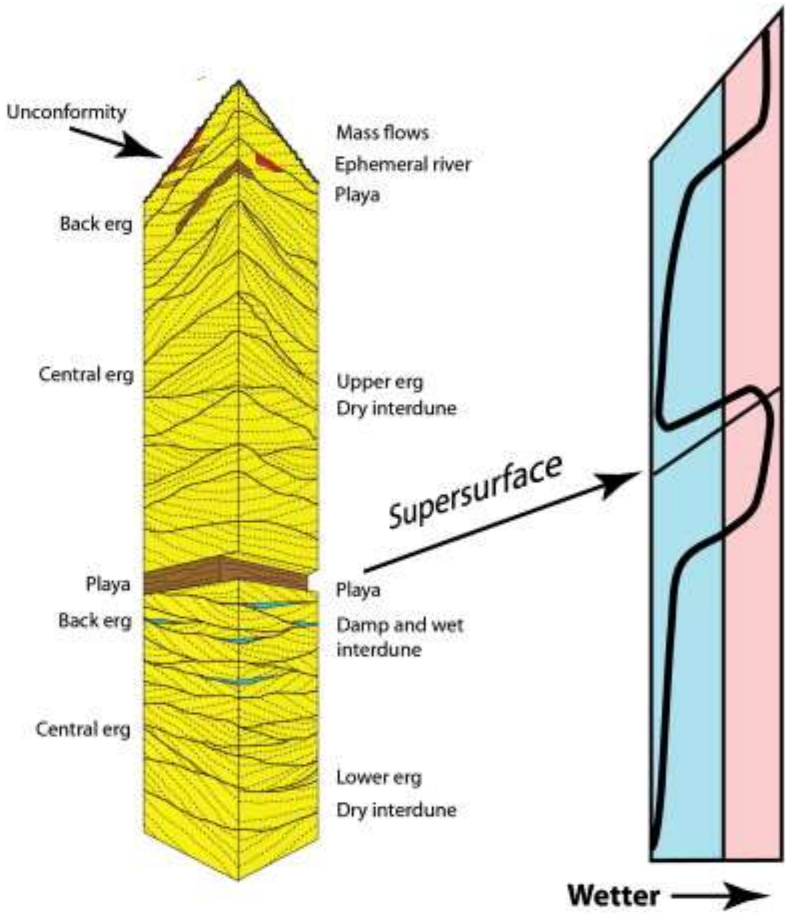

Fig. 16. Vertical section of the uppermost Makgabeng Formation. Note the development of damp and wet interdune facies association at the top of the lower erg and ephemeral-river, mass flow sandstone, and playa facies associations near the top of the upper erg. These intervals correspond to the overprint of periods of higher precipitation on the erg. Cartoon is not to scale, and wetness scale is a relative scale.

5. Discussion

The recognition of climatic impacts on sedimentation in the Precambrian has been limited to paleosols, specifically the composition of the paleoatmosphere (e.g. Ohmoto, 1996; Holland 1997, 2002; Rye and Holland, 1988; Prasad and Roscoe, 1996; Gutzmer and Beukes, 1998; Sheldon, 2006; Mossman et al., 2008; Driese et al., 2011; Crowe et al., 2013) and glaciogenic deposits (Williams and Schmidt, 1997; Young et al., 1998;

2001; Crowell, 1999; Martin, 1999; Schmidt and Williams, 1999; Ojakangas et al., 2001; Bindemand et al., 2010). The vertical succession of facies associations in the Makgabeng Formation indicates two periods of climatic amelioration during the history of the erg (Figs. 16 and 17).

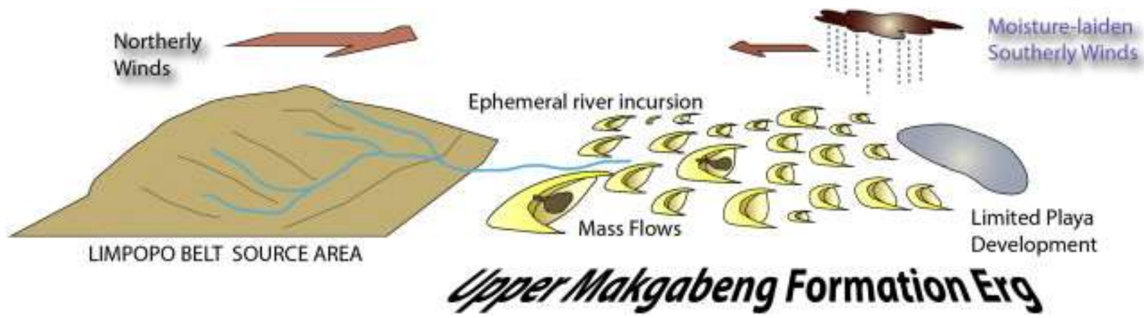

Fig. 17. Cartoon of possible sources of moisture and changes in moisture content across the termination of the Makgabeng erg.

The reduced availability of sand and higher water table induced by increasing precipitation mark the transition from dry to wet interdune deposits within the central- to back-erg facies of the Makgabeng Formation. Temporal changes in depositional environments have similarly been attributed to water table rises (e.g. Fryberger, 1990; Kocurek and Havholm, 1993; Uličný, 2004). The transition from the lower erg to the playa is marked by the presence of biological soil crust and is best interpreted as a super bounding surface related to stabilization of the land surface (see Kocurek, 1988). The biological soil crust represents the preservation of the upper part of an incipient soil horizon (Malenda et al., 2012; Simpson et al., 2013). Increases in water table levels permitted flooding on the super surface, preserved the biological soil crusts on the topographic highs, and developed the playa facies association. Variations in playa facies record seasonal and possibly longer-term decadal climatic changes. The end of playa sedimentation and the initiation of the upper erg indicates a shift back to less precipitation and restoration of the central erg system over the fore-erg. A caveat to this interpretation is that increased rainfall in the catchment area can allow progradation of dunes across a playa without necessarily occurring in the erg (Stone et al., 2010). The prevalence of 3rd -order surfaces indicates that a significant shift in wind direction occurred within the upper erg. That these shifting winds were coupled with increased precipitation is indicated by the appearance of mass flow sandstones that sculpted the dunes, ephemeral river deposits that impinged on the erg, and a high water table that permitted development of more localized playa deposits.

A test of climatic models via paleocurrent direction anaylsis of dune deposits has become important in understanding the validity of models (e.g. Parrish and Peterson, 1988; Loope and Rowe, 2003; Loope et al., 2004; Scherer and Goldberg, 2010). Loope and Rowe (2003) and Loope et al. (2004) recognized that increased amounts of rainfall on the Jurassic Navajo erg resulted in water table recharge and sustained fluvial flows into the interdune areas. These recognized transitions from arid to pluvial episodes are interpreted to record encroachment of the intertropical convergence zone into the core of the Navajo erg (Loope et al., 2004).

Paleomagnetic studies of the lower Waterberg formations indicate an approximate pole position of 39° north or south (Maré et al., 2006). This paleopole position is congruent with, if present, an intertropical convergence zone similar to the Navajo Sandstone. If this is the case, then the consistent wind direction followed by an eventual seasonal shift to a subordinate direction at 2.0 Gareflects the intertropical convergence zone and the development of a monsoonal wind shift coupled with an increase in precipitation.

5. Summary

- The Makgabeng Formation contains one of the oldest demonstrable records in Earth's history of the impact of climate changes on erg development in a continental dryland setting.
- The Makgabeng Formation consists of erg, interdune, playa or saline pan, mass-flow and ephemeral-river deposits. The lower and upper ergs were punctuated by development of a playa during a flooding phase. Interdune deposits display end-member damp and wet deposits.
- The vertical stacking of facies associations demonstrates a significant shift in amounts of precipitation that is reflected in changing water table levels as documented by bedding changes in interdune deposits and the appearance of ephemeral river and mass flow deposits late in the history of the erg.
- Changes in amounts of precipitation radically altered the Makgabeng Formation landscape through time.

Acknowledgements

This research was supported by the Kutztown University Undergraduate Research Committee, Kutztown University Research Committee, Kutztown University Foundation, and Kumba-Exxaro, the National Research Foundation, and the University of Pretoria in South Africa.

References

Allen, J.R.L., 1983. Studies of fluviatile sedimentation: bars, bar complexes and sandstone sheets (low sinuosity braided streams) in the Brownstones (L, Devonian), Welsh Borders. Sedimentary Geology 33, 237-293.

Allen, J.R.L., 1984. Sedimentary structures: Their character and physical basis. Elsevier, New York, v. 1, 593 pp.

Barton, Jr., J.M., Klemd, R., Zeh, A., 2006. The Limpopo Belt: a result of Archean to Proterozic Turkic-type orogenesis? In: Reimold, W.U., Gibson, R.L., (Eds.), Processes on the Early Earth. Geological Society of America Special Paper 405, pp. 315-332.

Benison, K.C., Goldstein, R.H., 2000. Sedimentology of ancient saline pans: an example from the Permian Opeche Shale, Williston Basin, North Dakota, U.S.A. Journal of Sedimentary Research 70, 159-169.

Billi, P., 2007. Morphology and sediment dynamics of ephemeral stream terminal distributary systems in the Kobo Basin (northern Welo, Ethiopia). Geomorphology 85, 98-113.

Bhattacharyya, A., Morad, S., 1993. Proterozoic braided ephemeral fluvial deposits; an example from the Dhandraul Sandstone Formation of the Kaimur Group, Son Valley, central India. Sedimentary Geology 84, 101-114.

Bindeman, I.N., Schmitt, A.K., Evans, D.A.D., 2010. Limits on hydrosphere-lithosphere interaction: Origin od the lowest know $\delta^{18}O$ silicate rock on Earth in the Paleoproterozoic Karlian rift. Geology 38, 631-634.

Bridge, J.S., 2003. Rivers and floodplains, forms, processes and sedimentary record. Blackwell, Oxford, U.K., 504 p.

Brookfield, M.E., 1977. The origin of bounding surfaces in ancient aeolian sandstones. Sedimentology 24, 303-332.

Bumby, A.J., 2000. The geology of the Blouberg Formation, Waterberg and Soutpansberg Groups in the area of Blouberg mountain, Northern Province, South Africa [PhD Dissertation}: University of Pretoria, Pretoria, South Africa, 331 p.

Bumby, A.J., Eriksson P.G., Van Der Merwe, R., 2004. The early Proterozoic sedimentary record in the Blouberg area, Limpopo Province, South Africa; implications for the timing of the Limpopo orogenic event. Journal of African Earth Sciences 39, 123-131.

Bumby, A.J., Eriksson P.G., Van Der Merwe, R., Brümmer, J.J., 2001. Shear-zone controlled basins in the Blouberg area, Northern Province, South Africa: syn- and post-tectonic sedimentation relating to ca. 2.0 Ga reactivation of the Limpopo Belt. Journal African Earth Sciences 33, 445-461.

Callaghan, C.C., Eriksson, P.G., Snyman, C.P., 1991. The sedimentology of the Waterberg Group in the Transvaal South Africa, an overview. Journal of African Earth Sciences 13, 121-139.

Chan, M.A., Archer, A.W., 1999. Spectral analysis of eolian foreset periodicities: implications for decadal-scale paleoclimatic oscillators. Paleoclimates 3, 239-255.

Chan, M.A., Archer, A.W., 2000. Cyclic eolian stratification on the Jurassic Navajo Sandstone, Zion National Park: Periodicities and implications for paleoclimate. In: Sprinkle, D.A., Chidsey, T.C., Anderson, P.B., (Eds.), Geology of Utah's Parks and Monuments, Utah Geological Association Publication 28, 607-617.

Corcoran, P.L., Bumby, A.J., Davis, D.W., 2013. The Paleoproterozoic Waterberg Group, South Africa: Provenance and its relation to the timing of the Limpopo orogeny. Precambrian Research 230, 45-60.

Cotter, E., 1978. The evolution of fluvial style, with special reference to the central Appalachians, In, Miall, A.D., Ed., Fluvial Sedimentology. Canadian Society of Petroleum Geologists Memior 5, Calgary, Alberta, 361-383.

Crowell, J.C., 1999. Pre-Mesozoic ice ages: their bearing on understanding the system. Geological Society of America Memoir 192, 106 p.

Crowe, S.A., Dressing, L.N., Beukes, N.J., Bau, M., Kruger, S.J., Frei, R., Canfield, D.E., 2013. Atmospheric oxidation three billion years ago. Nature 501, 535-538.

Davies, N.L., Gibling, M.R., 2010a. Cambrian to Devonian evolution of alluvial systems: the sedimentological impact of early land plants. Earth-Science Reviews 98, 171-200.

Davies, N.L., Gibling, M.R., 2010b. Paleozoic vegetation and the Siluro-Devonian rise of fluvial laterial accretion sets. Geology 38, 51-54.

Dorland, H.C., Beukes, N.J., Gutzmer, J., Evans, D.A.D., Armstrong, R.A., 2006. Precise SHRIMP U-Pb zircon age constraints on the lower Waterberg and Soutpansberg Groups, South Africa. South Africa Journal of Geology 109, 139-156.

Dott, R.H., Jr., 2003. The importance of eolian abrasion in supermature quartz sandstones and the paradox of weathering on vegetation-free landscapes. Journal of Geology 111, 387-405.

Driese, S.G., Jirsa, M.A., Ren, M., Brantley, S.L., Sheldon, N.D., Parker, D., Schmitz, M., 2011. Neoarchean paleoweathering of tonalite and metabasalt: implications for the reconstructions of 2.69 early terrestrial ecosystems and paleoatmosphic chemistry. Precambrian Research 189, 1-7.

Eglington, B.M., Armstrong, R.A., 2004. The Kaapvaal Craton and adjacent orogens, southern Africa: a geochronological database and overview of the geological development of the craton. South African Journal of Geology 107, 13-32.

Eriksson, K.A., Simpson, E.L., 1998. Controls on spatial and temporal distribution of Precambrian eolianites. Sedimentary Geology 120, 275-294.

Eriksson, P.G., Banerjee, S., Catuneanu, O., Corcoran, P.L., Eriksson, K.A., Hiatt, E.E., Laflamme, M., Lenhardt, N., Long, D.G.F., Miall, A.D., Mints, M.V., Pufahl, P.K., Sarkar, S., Simpson, E.L., Williams, G.E., 2013, Secular changes in sedimentation systems and sequence stratigaphy. Gondwana Research 24, 468-489.

Eriksson, P.G., Bumby, A.J., Brümmer, J.J., Van der Neut, M., 2006. Precambrian fluvial deposits: enigmatic palaeohydrological data from the c. 2-1.9 Ga Waterberg Group, South Africa. Sedimentary Geology 120, 5-53.

Eriksson, P.G., Cheney, E.S., 1992. Evidence for the transition to an Oxygen-rich atmosphere during the evolution of red beds in the Lower Proterozoic sequences of southern Africa. Precambrian Research 54, 257-269.

Eriksson, P.G., Long, D.G.F., Bumby, A.J., Eriksson, K.A., Simpson, E.L., Catuneanu, O., Claassen, M., Mtimkulu, Mudziri, K.T., M.N., Brümer, J.J., van der Neut, M., 2008. Palaeohydrological data from the 2.0-1.8 Ga Waterberg Group, South Africa: Discussion of a possible unique Palaeoproterozoic fluvial style. South African Journal of Geology 111, 183-206.

Eriksson, P.G., Porada, H., Banerjee, S., Bouougri, E., Sarkar, S., Bumby, A.J., 2007. 4 (c). Mat-destruction features. In: Schieber, J., Bose, P.K., Eriksson, P.G., Banerjee, S., Sarkar, A., Altermann, W., and Catuneanu, O., (Eds.), Atlas of microbial mats features preserved within the siliciclastic rock record. Atlases in Geosciences 2, Elsevier, New York, pp. 76-105.

Eriksson, P.G., Simpson, E.L., Eriksson, K.A. Bumby, A.J., Steyn, G.L., Sarkar, S., 2000. Muddy roll-up structures in clastic playa beds of the c. 1.8 Ga Waterberg Group, South Africa. Palaios 15, 177-183.

Frostick, L.E., Reid, I., 1977. The origin of horizontal laminae in ephemeral stream channel-fill. Sedimentology 24, 1-9.

Fryberger, S.G., 1990. Role of water in aeolian deposition. In: Fryberger, S.G., Krystinik, L.F., Schenk, C.J., (Eds.), Modern and ancient aeolian depositions: petroleum exploration and production. SEPM, Denver, CO, 5-1-5-11.

Fryberger, S.G., Al-Sari, A.M., Clisham, T.J., 1983. Eolian dune, interdune, and siliciclastic sabka sediments of an offshore prograding sand sea, Dhahran, Saudi Arabia. American Association of Petroleum Geologists Bulletin 67, 280-312.

Gierlowski-Kordesch, E., Rust, B.R., 1994. The Jurassic East Berlin Formation, Hartford Basin, Newark Supergroup (Connecticut and Massachusetts). In: In: Renaut, R.W., Last, W.M., (Eds.), Sedimentology and geochemistry of modern and ancient saline lakes. Society for Sedimentary Geology Special Publication 50, p 249-268.

Gradziński, R., Gagol, J., Ślaczka, A., 1979. The Tumlin Sandstone (Holy Cross Mts., Central Poland): Lower Triassic deposits if aeolian dunes and interdune areas. Acta Geologica Polonica 29, 151-175.

Gradziński, R., Uchman, A., 1994. Trace fossils from interdune deposits – an example the Lower Triassic aeolian Tumlin Sandstone, central Poland. Palaeogeography, Paloeoclimatology, Palaeoecology 108, 121-138.

Gutzmer, J., Beukes, N.J., 1998. Earliest laterites and possible evidence for terrestrial vegetation in the Early Proterozoic. Geology 26, 263-266.

Handford, C.R., 1982. Sedimentology and evaporite genesis in a Holocene continental-sabkha playa basin – Bristol Dry Lake, California. Sedimentology 29, 239-253.

Hanson, R.E., Gose, W.A., Crowley, J., Ramezani, S.A., Bowring, D.S., Hall, R.P., Pancake, J.A., Mukwakwami, J., 2004. Paleoproterozoic intraplate magmatism and basin development on the Kaapvaal Craton: Age, paleomagnetism and geochemistry of ~1.93-~1.87 Ga post Waterberg dolerites. South African Journal of Geology 107, 233-254

Harms, J.C., Southard, J.B., Walker, R.G., 1982. Structures and sequences in clastic rocks. SEPM (Society for Sedimentary Geology) Short Course 9, Tulsa, OK, pp. 251.

Holland, H., 1997. Evidence in pre-2.2 paleosols for the early evolution of atmospheric oxygen and terrestrial biota: discussion and reply. Geology 25, 857-859.

Holland, H., 2002. Volcanic gases, black smokers, and the Great Oxidation Event. Geochimica et Cosmochemica Acta 66, 3811-3826.

Holliday, V.T., Mayer, J.H., Fredlund, G.G., 2008. Late Quaternary sedimentology and geochronology of small playas on the Southern High Plains, Texas and New Mexico, U.S.A. Quaternary Research 70, 11-25.

Hunter, R.E. 1977. Basic types of stratification in small eolian dunes. Sedimentology 24, 361-387.

Hunter, R.E., 1981. Stratification styles in sandstones: Some Pennsylvanian to Jurassic examples from the western interior U.S.A. In: Ethridge, F.G., Flores, R.M., (Eds.) Recent and ancient nonmarine depositional environments. Society of Economic Paleontologists and Mineralogists Special Publication 31, pp. 315-329.

Hunter, R.E., Richmond, B.M., 1988. Daily cycles in coastal dunes. Sedimentary Geology 55, 43-67.

Jansen, H., 1982. The geology of the Waterberg basin in the Transvaal, Republic of South Africa. Geological Survey of South Africa Memoir 71, 98 p.

Kröner, A., Jaeckel, P., Brandl, G., Nechin, A.A., Pidgeon, R.T., 1999. Single zircon ages for granitoid gneisses in the Central Zone of the Limpopo Belt, southern Africa and geodynamic significance. Precambrian Research 93, 299-337.

Kocurek, G., 1981. Significance of interdune deposits and bounding surfaces in aeolian dune sands. Sedimentology 28, 753-780.

Kocurek, G., 1988. First-order and super bounding surfaces in eolian sequences – bounding surfaces revisited. Sedimentary Geology 56, 193-206

Kocurek, G., 1991. Interpretation of ancient aeolian sand dunes. Annual Review Earth and Planetary Sciences 19, 43-75.

Kocurek, G., Dott, R.H., 1981. Distinction and use of stratification types in the interpretation of eolian sand. Journal of Sedimentary Petrology 51, 579-595.

Kocurek, G., Havholm, K.G., 1993. Eolian sequence stratigraphy – a conceptual framework. In: Weimer, P., Posamentier, H.W., (Eds.), Siliciclastic sequence stratigraphy: Recent developments and applications. American Association of Petroleum Geology Memoir 58, p. 393-409.

Kocurek, G., Lancaster, N., 1999. Aeolian system sediment state: Theory and Mojave Desert Kelso dune field example. Sedimentology 46, 505-515.

Lancaster, N., 1997. Response of eolian geomorphic systems to minor climate change: examples from the southern California deserts. Geomorphology 19, 333-347.

Lancaster, N., Teller, J.T., 1988. Interdune deposits of the Namib Sand Sea. Sedimentary Geology 55, 91-107.

Langford, R.P., 1989. Fluvial-aeolian interactions: Part I. Modern systems. Sedimentology 36, 1023-1035.

Langford, R.P., Chan, M.A., 1989. Fluvial-aeolian interactions: Part II. Ancient systems. Sedimentology 36, 1037-1051.

Langston, G., McKenna Neuman, C., 2005. An experimental study on the susceptibility of crusted surfaces to wind erosion: A comparison of the strength of properties of biotic and salt crusts. Geomorphology 72, 40-53.

Last, W.M., 1989. Sedimentology of a saline playa in northern Great Plains, Canada. Sedimentology 36, 109-123.

Last, W.M., 2002. Limnology of salt lakes. Geosciences Journal 6, 347-369.

Light, M.P.R., 1982. The Limpopo Belt: a result of continental collision. Tectonics 1, 325-342.

Long, D.G.F., 2011. Architecture and depositional style of fluvial systems before land plants: a comparison of Precambrian, early Paleozoic and modern fluvial systems. In: Davidson, S.K., Leleu, S., North, C.P., (Eds.), From river to rock record: The preservation of fluvial sediments and their subsequent interpretation. Society of Economic Paleontologists and Mineralogists Special Publication 97, pp. 37-61.

Loope, D.B., Dingus, L., Swisher, C.C. III, Minjin, C., 1998. Life and death in a Late Cretaceous dune field, Nemegt basin, Mongolia. Geology 26, 27-30.

Loope, D.B., Mason, J.A., Dingus, L., 1999. Lethal landslides from eolian dunes. Journal of Geology 53, 707-713.

Loope, D.B., Rowe, C.M., 2003. Long-lived pluvial episodes during deposition of the Navajo Sandstone. Journal of Geology 111, 223-232.

Loope, D.B., Rowe, C.M., Joeckel, R.M., 2001. Annual monsoon rains recorded by Jurassic dunes. Nature 422, 64-66.

Loope, D.B., Simpson, E.L., 1992. Significance of thin sets of eolian cross-strata. Journal of Sedimentary Petrology 62, 849-859.

Loope, D.B., Steiner, M.B., Rowe, C.M., Lancaster, N., 2004. Tropical westerlies over Pangaean sand seas. Sedimentology 51, 315-322.

Loope, D.B., Swinehart, J.B., Mason, J.P., 1995. Dune-dammed paleovalleys of the Nebraska Sand Hills: Intrinsic versus climatic controls on the accumulation of lake and marsh sediments. Geological Society of American Bulletin 107, 396-406.

Lowenstein, T.K., Hardie, L.A., 1985. Criteria for the recognition of salt-pan evaporates. Sedimentology 32, 627-644.

Malenda, H.F., Simpson, E.L., Wizevich, M.C., Tindall, S.E., 2012. Towards the recognition of biological soil crusts in the rock record: Key features from the study of modern and Cretaceous examples. In: Noffke, N., Chafetz, H., (Eds.), Microbial Mats in siliciclastic depositional systems through time. SEPM (Society of Sedimentary Geology) Special Publication 101, 125-138.

Maré, L.P., Eriksson, P.G., Améglio, L., 2006. A paleomagnetic study of the lower part of the Paleoproterozoic Waterberg Group, South Africa. Journal of African Earth Sciences 44, 21-36.

Marín, L., Forman, S.L.,Valdez, A., Bunch, F., 2005. Twentieth century dune migration at the Great Sand Dunes National Park and Preserve, Colorado, relation to drought and variability. Geomorphology 70, 163-183.

Martin, D.McB., 1999. Depositional setting and implications of Paleoproterozoic glaciomarine sedimentation in the Hamersley Province, Western Australia. Geological Society of America Bulletin 111, 189-203.

Meinster, B., Tickell, S.J., 1975. Precambrian aeolian deposits in the Waterberg Supergroup. Transactions of the Geological Society of South Africa 78, 191-200.

Mossman, D.J., Minter, W.E.L., Dutkiewicz, A., Hallbauer, D.K., George, S.C., Hennigh, Q., Reimer, T.O., Horscroft, F.D., 2008. The indigenous origin of Witwatersrand "carbon". Precambrian Research 164, 173-186.

Mountney, N., Howell, J., Flint, S., Jerrain, D., 1999. Relating eolian bounding – surface geometries to the bedforms that generated them: Etjo Formation Cretaeous, Namiba. Geology 27, 159-162.

Mountney, N.P., Jagger, A., 2004. Stratigraphic evolution of an aeolian erg margin system: The Permian Cedar Mesa Sandstone, SE Utah, USA. Sedimentology 51, 713-743.

Ohmoto, H., 1996, Evidence in pre-2.32 Ga paleosols for the early evolution of atmospheric oxygen and terrestrial biota. Geology 24, 1135-1138.

Ojakangas, R.W., Marmo, J.S., Heiskanen, K.I., 2001. Basin evolution of the Paleoproterozoic Karelian Supergroup of the Fennoscandian (Baltic) Shield. Sedimentary Geology 141-142, 255-285.

Parrish, J.T., Peterson, F., 1988. Wind directions predicted from global circulation models and wind directions determined from aeolian sandstones of the western United States. Sedimentary Geology 56, 261-282.

Peterson, F., 1988. Pennsylvanian to Jurassic aeolian transport systems in the western United States. Sedimentary Geology 56, 207-260.

Porada, H., Eriksson, P.G., 2009. Cyanobacterial mat features preserved in the siliciclastic sedimentary record: Paleodeserts and modern supratidal flats. In: Seckbach, J., Walsh, M., (Eds.). From Fossils to Astrobiology: Records of life on Earth and search for extraterrestrial biosignatures. Cellular Origin, Life in Extreme Habitats and Astrobiology 12, pp. 181-210.

Porter, M.L., 1986. Sedimentary record of erg migration. Geology 14, 497-500.

Porter, M.L., 1987. Sedimentology of an ancient erg margin: T he Lower Jurassic Aztec Sandstone, southern Nevada and southern California. Sedimentology 34, 661-680.

Prasad, N., Roscoe, S.M., 1996. Evidence of anoxic to oxic atmospheric change during 2.45-2.22 Ga from lower and upper sub-Huronian paleosols, Canada. Cantena 27, 105-121.

Pulvertaft, T.C.R., 1985. Aeolian dune and wet interdune sedimentation in the Middle Proterozoic Dala Sandstone, Sweden. Sedimentary Geology 44, 93-111.

Reinhardt, L., Ricken, W., 2000. The stratigraphic and geochemical record of playa cycles: Monitoring a Pangaean monsoon-like system (Triassic, Middle Keuper, S. Germany). Palaeogeography, Palaeoclimatology, Palaeoecology 161, 205-227.

Roering, C., van Reenen, D.D., Smit, C.A., Barton Jr., J.M., De Beer, J.H., De Wit, M.J., Stettler, E.H., Van Schalkwyk, J.F., Stevens, G., Pretorius, S., 1992. Tectonic model for the evolution of the Lompopo Mobile Belt. Precambrian Research 55, 539-552.

Rubin, D.M., Carter, C.L., 2006. Bedforms and cross bedding in animation. SEPM (Society of Sedimentary Geology) Atlas Series No. 2.

Rubin, D.M., Hunter, R.E., 1982. Bedform climbing in theory and nature. Sedimentology 29, 121-138.

Rubin, D.M., Hunter, R.E., 1983. Reconstructing bedform assemblages from compound cross bedding, In:, Brookfield, M.E., Ahlbrandt, T.S., eds., Eolian sediments and processes. Developments in Sedimentology 38, 407-427.

Rye, R., Holland, H., 1988. Paleosols and the evolution of atmospheric oxygen: a critical review. American Journal of Science 298, 621-672.

S.A.C.S. (South African Committee for Stratigraphy), 1980. Stratigraphy of South Africa. Part 1 (Compiler L.E. Kent). Lithostratigraphy of the Republic of South Africa, South West

Africa/Namibia and the Republics of Boputhatswana, Transkei and Venda. Handbook Geological Survey of South Africa 8, Pretoria, 690 p.

Scherer, C.M.S., Goldberg, K., 2010. Cyclic cross-bedding in the eolian dunes of the Sergi Formation (Upper Jurassic) Recôncavo Basin: Inferences about the wind regime. Palaeogeography, Palaeoclimatology, Palaeoecology 296, 103-110.

Schmidt, P.W., Williams, G.E., 1999. Paleomagnetism of the Paleoproterozoic hematitic breccia and paleosol at Ville-Marie, Québec: Further evidence for low paleolatitude of Huronian glaciation. Earth and Planetary Science Letters 172, 273-285.

Sheldon, N.D., 2006. Precambrian paleosols and atmospheric CO2 levels. Precambrian Research 147, 148-155.

Simpson, E.L., Bose, P., Alkmim, F.F., Rainbird, R., Martins-Neto, M., Bumby, A., Eriksson, P.G., Eriksson, K.A., Middleton, L., 2004. Oldest eolian deposits, earliest 1.8 Ga ergs and Proterozoic erg dynamics. In: Eriksson, P.G., Alterman, W., Nelson, D., Mueller, W., Catuneanu, O., (Eds.), The Precambrian Earth: Tempos and Events. Developments in Precambrian Geology 12, Elsvier, Amsterdam. pp. 642-657.

Simpson, E.L., Eriksson, K.A., Kuklis, C.A., Eriksson, P.G., Bumby, A.J., Jaarsveld, C.F., 2004. Saline pan deposits, the ~1.8 Makgabeng Formation, Waterberg Group, South Africa. Sedimentary Geology 163, 279-292.

Simpson, E.L., Eriksson, K.A., Eriksson, P.G., Bumby, A.J., 2002. Eolian dune degradation and generation of massive sandstones in the Paleoproterzoic Makgabeng Formation, Waterberg Supergroup, South Africa. Journal of Sedimentary Research 72, 40-45.

Simpson, E.L., Eriksson, K.A., Mueller, W.U., 2012. 3.2 Ga eolian deposits from the Moodies Group, Barberton Greenstone Belt, South Africa: Implications form the origin of first cycle quartz sandstones. Precambrian Research 214-215, 185-191.

Simpson, E.L., Heness, E.A., Bumby, A.J., Eriksson, P.G., Eriksson, K.A., Hilbert-Wolf, H.L., Linnevelt, S., Fitzgerald Malenda, H., Modungwa, T., Okafor, O.J., 2013. 2.0 Ga continental microbial diversity in a paleodesert setting. Precambrian Research, v. 237, 36-50.

Smoot, J.P., Castens-Seidell, B., 1994. Sedimentary features produced by efflorescent salt crusts, Saline Valley and Death Valley, California. In: Renaut, R.W., Last, W.M., (Eds.), Sedimentology and geochemistry of modern and ancient saline lakes. Society for Sedimentary Geology Special Publication 50, p. 73-90.

Stone, A.E.C., Thomas, D.S.G., Viles, H.A., 2010. Late Quaternary palaeohydrological changes in the northern Namib Sand Sea: New chronologies using OSL dating of interdigitated aeolian and water-lain interdune deposits. Palaeogeography, Palaeoclimatology, Palaeoecology 288, 35-53.

Svendsen, J., Stollhofen, H., Krapf, C.B.E., Stanistreet, I.G., 2003. Mass and hyperconcentrated flow deposits record dune damming and catastrophic breakthrough of ephemeral rivers, Skeleton Coast Erg, Nambia. Sedimentary Geology 160, 7-31.

Sweeny, M.R., Loope, D.B., 2001. Holocene dune-sourced alluvial fans in the Nebraska Sand Hills. Geomorphology 38, 31-46.

Tooth, S., 2000. Process, form, and change in dryland rivers: A review of recent research. Earth Science Reviews 51, 67-107.

Turner, B.R., Smith, D.B., 1997. A playa deposit of pre-Yellow Sands age (upper Rotliegend/Weissliegend) in the Permian of northeast England. Sedimentary Geology 114, 305-319.

Uličný, D., 2004. A drying-upward aeolian system of the Bohdašín Formation (Early Triassic), Sudetes of NE Czech Republic: Recors of seasonality and long-term palaeoclimate change. Sedimentary Geology 167, 17-39.

Walraven, F., Hattingh, E., 1993. Geochronology of the Nebo granite, Bushveld Complex. South African Journal of Geology 96, 31-41.

Williams, G.E., 1971. Flood deposits of the sand-bed ephemeral streams of central Australia. Sedimentology 17, 1-40.

Williams, G.E., Schmidt, P.W., 1997. Paleomagnetism of the Paleoproterozoic Gowganda and Lorrain formations, Ontario: low paleolatitude for Huronian glaciation. Earth and Planetary Science Letters 153, 157-169.

Wilson, I.G., 1972. Aeolian bedforms – their development and origins. Sedimentology 19, 173-210.

Wizevich, M.C., 1997. Fluvial-eolian deposits in Devonian New Mountain Sandstone, Table Mountain, Southern Victoria Land, Antarctica: Sedimentary architecture, genesis and stratigraphic evolution, In: Ricci, C.A., (Ed.), The Antarctic region: Geological evolution and processes. Terra Antarctica Publications, Siena, Italy, 933-944.

Young, G.M., von Brunn, V., Gold, D.J.C., Minter, W.E.L., 1998. Earth's oldest reported glaciation: Physical and chemical from the Archean Mozaan Group (2.9 Ga) of South Africa. Journal of Geology 106, 523-538.

Young, G.M., Long, D.G.F., Fedo, C.M., Nesbitt, H.W., 2001, Paleoproterozoic Huronian basin: product of Wilson cycle punctuated by glaciations and meteorite impact. Sedimentary Geology 141-142, 233-254.